Table 1. Cytotoxicity of clones from HBV transgenic mice immunized with HBsAg and α-GalCer

	Mouse	Specific cytotoxicity (%)	
		E:T = 20:1	E:T = 4:1
Clone T-1	Transgenic	42.2	21.8
Clone T-2	Transgenic	17.8	10.5
Clone T-3	Transgenic	36.8	2.5

HBsAg-specific CTL clones were established by limiting dilution and the cytolytic activity of HBsAg specific was assessed using a Europium release assay. The details are described in Methods.

Table 2. Analysis of HBsAg-specific CTL precursor frequency

Mouse	Immunization	Rate of cell proliferation	HBsAg positive
HBV Tg	HBsAg	4/960	0/4
HBV Tg	HBsAg + α-GalCer	99/960	88/99

The CD8-positive cells (three cells per well) isolated by using MACS system were cultured in 96-well plates with MMC-treated spleen cells (4×10^5 per well) and MMC-treated P815preS1 (2×10^4 per well) in complete RPMI 1640. The cells were re-stimulated with MMC-treated spleen cells and P815preS1 every 7 days. After 14 days, the number of wells in which the cells proliferated was counted and the proportion of HBsAg-specific CTLs was measured by flow cytometric analysis on a FACScan.

immunization method and to elucidate its mechanisms for the tolerance break, studies need to be performed under physiological conditions. Therefore, we performed the experiments using HBsAg transgenic mice, the model of the HBV carriers.

Previous study demonstrated that α-GalCer activated intrahepatic NKT cells to secrete antiviral cytokines (IFN-γ and IFN-α/β) in the liver and had the potential to control viral replication during natural HBV infection (18). Recently, another studies reported that antigen-specific CTLs were remarkably induced when antigen was administrated together with α-GalCer by the intra-nasal route (25, 26). Therefore, we evaluated the effect of activated NKT cells on the induction of HBsAg-specific CTL by administering α-GalCer. Indeed, we found that the activation of $V\alpha14^+$ NKT cells by α-GalCer strongly enhanced the efficiency of CTL induction in the $V\alpha14^+$ NKT WT mice, whereas this did not occur in the $V\alpha14^+$ NKT KO mice. Frequency analysis clearly showed that activated $V\alpha14^+$ NKT cells increase the number of HBsAg-specific $CD8^+$ T cells. Furthermore, the enhancement of CTL induction efficiency was observed not only in non-transgenic mice but also in HBsAg transgenic mice.

After the immunization with HBsAg and α-GalCer, the elevation of serum alanine aminotransferase (ALT) was observed in HBsAg transgenic mice (ALT levels; 5061 ± 1071 IU l^{-1}) but not in non-transgenic mice. Furthermore, we confirmed no liver injury in Jα18 KO mice/HBsAg transgenic mice immunized with HBsAg and α-GalCer (data not shown). Thus, the activation of NKT cells induced the liver injury in HBsAg transgenic mice after α-GalCer injection. HBsAg transgenic mice (lineage 107-5D) used in this study are consistently more sensitive to LPS or inflammatory cytokine (i.e. IFN-γ and TNF-α) compared with other HBV Tg mice lineage (27). Therefore, severe liver injury in these HBsAg transgenic mice was caused by cytokines produced by α-GalCer-activated NKT cells. Other reports have indicated that α-GalCer was not toxic in human including liver injury (28–30). However, our data suggested the fear of severe liver injury in patients with chronic HBV infection. The kinetics of ALT, which started to rise just after the immunization and declined within several days, also supports the idea above. The CTLs induced by the immunization might have the potential to cause liver damage. However, from the kinetics of ALT levels, it is unlikely that those CTLs contributed the ALT elevation in this case. It may be explained by HBsAg down-regulation, which was caused by the effect of IFN-γ and TNF-α (8, 9). Moreover, previous report demonstrated that HBV-specific CTLs profoundly suppress hepatocellular HBV gene expression in HBV transgenic mice by a non-cytolytic process (8, 9). Thus, the CTL induction was very meaningful for HBV clearance even if the destruction of the HBV-infected hepatocytes is induced by the CTLs. On the other hand, Mancini *et al.* (31) have reported that HBV DNA immunization successfully broke B- and T cell unresponsiveness to viral antigens in HBV transgenic mice, but these antigen-specific immune responses did not cause an increase in transaminase activity. We have not studied if this phenomenon is applicable in our model; however, further study including the detailed analysis of *in vitro* and *in vivo* function of CTLs induced from the tolerant mice will be necessary.

Next, we examined the effect of blocking cytokines and CD40L with neutralizing antibodies *in vivo*. Our results suggested that IL-4, TNF-α and CD40/CD40L are important for CTL induction in the case of HBsAg alone and that IL-2 and CD40L are essential for the enhancement of CTL induction in the case of HBsAg and α-GalCer co-immunization. In addition, it was proved that the enhancing effect of α-GalCer on CTL induction could be substituted by IL-2 and CD40L in the HBsAg immunization experiment. As shown in Fig. 5, the frequency of HBsAg-specific $CD8^+$ T cells in CTL lines and IL-2 production from the mice immunized with HBsAg and once α-GalCer was higher than those from the mice immunized with HBsAg and three times α-GalCer. These data indicated that the enhancement of IL-2 production is critical for CTL induction in the case of HBsAg and α-GalCer co-immunization.

In the splenocytes of the mice administered with α-GalCer, we found that the expression of cytokine mRNAs was strongly enhanced and that the enhancement of mRNA expression was observed not only in NKT cells but also in $CD4^+$ and $CD8^+$ T cells. IL-2 mRNA expression was enhanced in all the analyzed cell fractions. In particular, $CD4^+$ T cells mainly produced IL-2 in activation of NKT cells and expression of CD40L on $CD4^+$ T cells constitutively was important for CTL induction. It was previously reported that CTL responses require the activate involvement of $CD4^+$ T cells (32, 33). Moreover, activated NKT cells stimulate the full maturation of DCs, and this maturation accounts for the induction of combined T_h1 and $CD8^+$ T cell immunity to a co-administered protein (34).

As demonstrated previously (35), the administration of α-GalCer strongly enhanced the expression of mRNAs encoding cytokines, including IFN-γ, TNF-α, IL-2 and IL-4, which are known to affect CTL induction and proliferation (36–39). On the other hand, a CD40/CD40L signal is known to play a critical role in the NKT–DC interaction (40–42), and production of IFN-γ but not IL-4 by NKT cells requires a CD40/CD40L signal (42). It is also suggested that monocyte-derived DCs generated in the presence of IL-15 can express IL-2 on activation with CD40L. IL-2 and IL-15 are reported to play an important role in the acquired immune response to foreign pathogens (43). We think that our results are consistent with these reports and that they support our results that IL-2 and CD40–CD40L interaction play the key role on the induction of CTL response.

In the current studies, we showed that CTL tolerance in HBsAg transgenic mice can be broken by the activation of $V\alpha14^+$ NKT cells. Although the cytotoxic activity and proliferation of HBsAg-specific CTLs from the HBsAg transgenic mice were lower than those from WT mice, they were apparently induced in the transgenic mice. In addition, by using limiting dilution analysis, we confirm that HBsAg-specific CTL precursor cells are present relatively frequently in the spleen of HBsAg transgenic mice treated with HBsAg and α-GalCer. Persistent HBV infection is characterized by a lack of or a weak CTL response to HBV; however, our findings suggested that this weak CTL response can be enhanced or that CTL tolerance can be broken by the activation of NKT cells. We think that it can be applied to the therapeutic purpose, suppressing HBV replication by inducing effective CTL response. We also think that it may explain the mechanism for the development of CH from asymptomatic status in human HBV carriers.

We conclude that the activation of NKT cells strongly promotes the proliferation of HBsAg-specific CTLs through production of a high level of IL-2 and that this enables the induction of CTLs even in HBsAg transgenic mice. These results may open up a new method for clearing the virus from patients with persistent HBV infection.

Acknowledgements

We are grateful to Francis V. Chisari for providing HBsAg transgenic mice lineage 107-5D and the HBsAg-specific $CD8^+$ CTL clone 6C2.

Abbreviations

ALT	alanine aminotransferase
ASC	asymptomatic carrier
cDNA	complementary DNA
CH	chronic hepatitis
DC	dendritic cell
α-GalCer	alpha-galactosylceramide
HBV	hepatitis B virus
KO	knockout
MMC	mitomycin C
RT	reverse transcription
TNF	tumor necrosis factor
WT	wild-type

References

1 Boni, C., Penna, A., Ogg, G. S. *et al.* 2001. Lamivudine treatment can overcome cytotoxic T-cell hyporesponsiveness in chronic hepatitis B: new perspectives for immune therapy. *Hepatology.* 33:963.
2 Binder, D. and Kundig, T. M. 1991. Antiviral protection by CD8+ versus CD4+ T cells. CD8+ T cells correlating with cytotoxic activity *in vitro* are more efficient in antivaccinia virus protection than CD4-dependent IL. *J. Immunol.* 146:4301.
3 Eichelberger, M., Allan, W., Zijlstra, M., Jaenisch, R. and Doherty, P. C. 1991. Clearance of influenza virus respiratory infection in mice lacking class I major histocompatibility complex-restricted CD8+ T cells. *J. Exp. Med.* 174:875.
4 Hou, S., Doherty, P. C., Zijlstra, M., Jaenisch, R. and Katz, J. M. 1992. Delayed clearance of Sendai virus in mice lacking class I MHC-restricted CD8+ T cells. *J. Immunol.* 149:1319.
5 Chisari, F. V., Filippi, P., McLachlan, A. *et al.* 1986. Expression of hepatitis B virus large envelope polypeptide inhibits hepatitis B surface antigen secretion in transgenic mice. *J. Virol.* 60:880.
6 Ando, K., Moriyama, T., Guidotti, L. G. *et al.* 1993. Mechanisms of class I restricted immunopathology. A transgenic mouse model of fulminant hepatitis. *J. Exp. Med.* 178:1541.
7 Ando, K., Guidotti, L. G., Cerny, A., Ishikawa, T. and Chisari, F. V. 1994. CTL access to tissue antigen is restricted *in vivo*. *J. Immunol.* 153:482.
8 Guidotti, L. G., Ando, K., Hobbs, M. V. *et al.* 1994. Cytotoxic T lymphocytes inhibit hepatitis B virus gene expression by a noncytolytic mechanism in transgenic mice. *Proc. Natl Acad. Sci. USA.* 91:3764.
9 Guidotti, L. G., Ishikawa, T., Hobbs, M. V., Matzke, B., Schreiber, R. and Chisari, F. V. 1996. Intracellular inactivation of the hepatitis B virus by cytotoxic T lymphocytes. *Immunity* 4:25.
10 Ando, K., Hiroishi, K., Kaneko, T. *et al.* 1997. Perforin, Fas/Fas ligand, and TNF-alpha pathways as specific and bystander killing mechanisms of hepatitis C virus-specific human CTL. *J. Immunol.* 158:5283.
11 Gremion, C., Grabscheid, B., Wolk, B. *et al.* 2004. Cytotoxic T lymphocytes derived from patients with chronic hepatitis C virus infection kill bystander cells via Fas-FasL interaction. *J. Virol.* 78:2152.
12 Bendelac, A., Rivera, M. N., Park, S. H. and Roark, J. H. 1997. Mouse CD1-specific NK1 T cells: development, specificity, and function. *Annu. Rev. Immunol.* 15:535.
13 Makino, Y., Kanno, R., Ito, T., Higashino, K. and Taniguchi, M. 1995. Predominant expression of invariant V alpha 14+ TCR alpha chain in NK1.1+ T cell populations. *Int. Immunol.* 7:1157.
14 Cui, J., Shin, T., Kawano, T. *et al.* 1997. Requirement for Valpha14 NKT cells in IL-12-mediated rejection of tumors. *Science.* 278:1623.
15 Kita, H., Moriyama, T., Kaneko, T. *et al.* 1993. HLA B44-restricted cytotoxic T lymphocytes recognizing an epitope on hepatitis C virus nucleocapsid protein. *Hepatology.* 18:1039.
16 Cerny, A., McHutchison, J. G., Pasquinelli, C. *et al.* 1995. Cytotoxic T lymphocyte response to hepatitis C virus-derived peptides containing the HLA A2.1 binding motif. *J. Clin. Invest.* 95:521.
17 Schirmbeck, R., Bohm, W., Ando, K., Chisari, F. V. and Reimann, J. 1995. Nucleic acid vaccination primes hepatitis B virus surface antigen-specific cytotoxic T lymphocytes in nonresponder mice. *J. Virol.* 69:5929.
18 Kakimi, K., Guidotti, L. G., Koezuka, Y. and Chisari, F. V. 2000. Natural killer T cell activation inhibits hepatitis B virus replication *in vivo*. *J. Exp. Med.* 192:921.
19 Kojo, S., Seino, K., Harada, M. *et al.* 2005. Induction of regulatory properties in dendritic cells by Valpha14 NKT cells. *J. Immunol.* 175:3648.
20 Wirth, S., Guidotti, L. G., Ando, K., Schlicht, H. J. and Chisari, F. V. 1995. Breaking tolerance leads to autoantibody production but not autoimmune liver disease in hepatitis B virus envelope transgenic mice. *J. Immunol.* 154:2504.
21 Shimizu, Y., Guidotti, L. G., Fowler, P. and Chisari, F. V. 1998. Dendritic cell immunization breaks cytotoxic T lymphocyte tolerance in hepatitis B virus transgenic mice. *J. Immunol.* 161:4520.
22 Rice, J., Buchan, S., Dewchand, H., Simpson, E. and Stevenson, F. K. 2004. DNA fusion vaccines induce targeted epitope-specific CTLs against minor histocompatibility antigens from a normal or tolerized repertoire. *J. Immunol.* 173:4492.

23 Paczesny, S., Banchereau, J., Wittkowski, K. M., Saracino, G., Fay, J. and Palucka, A. K. 2004. Expansion of melanoma-specific cytolytic CD8+ T cell precursors in patients with metastatic melanoma vaccinated with CD34+ progenitor-derived dendritic cells. *J. Exp. Med.* 199:1503.
24 Sette, A. D., Oseroff, C., Sidney, J. *et al.* 2001. Overcoming T cell tolerance to the hepatitis B virus surface antigen in hepatitis B virus-transgenic mice. *J. Immunol.* 166:1389.
25 Ko, S. Y., Ko, H. J., Chang, W. S., Park, S. H., Kweon, M. N. and Kang, C. Y. 2005. Alpha-galactosylceramide can act as a nasal vaccine adjuvant inducing protective immune responses against viral infection and tumor. *J. Immunol.* 175:3309.
26 Youn, H. J., Ko, S. Y., Lee, K. A. *et al.* 2007. A single intranasal immunization with inactivated influenza virus and alpha-galactosylceramide induces long-term protective immunity without redirecting antigen to the central nervous system. *Vaccine.* 25:5189.
27 Gilles, P. N., Guerrette, D. L., Ulevitch, R. J., Schreiber, R. D. and Chisari, F. V. 1992. HBsAg retention sensitizes the hepatocyte to injury by physiological concentrations of interferon-gamma. *Hepatology.* 16:655.
28 Veldt, B. J., van der Vliet, H. J., von Blomberg, B. M. *et al.* 2007. Randomized placebo controlled phase I/II trial of alpha-galactosylceramide for the treatment of chronic hepatitis C. *J. Hepatol.* 47:356.
29 Giaccone, G., Punt, C. J., Ando, Y. *et al.* 2002. A phase I study of the natural killer T-cell ligand alpha-galactosylceramide (KRN7000) in patients with solid tumors. *Clin. Cancer Res.* 8:3702.
30 Ishikawa, A., Motohashi, S., Ishikawa, E. *et al.* 2005. A phase I study of alpha-galactosylceramide (KRN7000)-pulsed dendritic cells in patients with advanced and recurrent non-small cell lung cancer. *Clin. Cancer Res.* 11:1910.
31 Mancini, M., Hadchouel, M., Davis, H. L., Whalen, R. G., Tiollais, P. and Michel, M. L. 1996. DNA-mediated immunization in a transgenic mouse model of the hepatitis B surface antigen chronic carrier state. *Proc. Natl Acad. Sci. USA.* 93:12496.
32 Keene, J. A. and Forman, J. 1982. Helper activity is required for the *in vivo* generation of cytotoxic T lymphocytes. *J. Exp. Med.* 155:768.
33 Cardin, R. D., Brooks, J. W., Sarawar, S. R. and Doherty, P. C. 1996. Progressive loss of CD8+ T cell-mediated control of a gamma-herpesvirus in the absence of CD4+ T cells. *J. Exp. Med.* 184:863.
34 Fujii, S., Shimizu, K., Smith, C., Bonifaz, L. and Steinman, R. M. 2003. Activation of natural killer T cells by alpha-galactosylceramide rapidly induces the full maturation of dendritic cells *in vivo* and thereby acts as an adjuvant for combined CD4 and CD8 T cell immunity to a coadministered protein. *J. Exp. Med.* 198:267.
35 Ito, H., Ando, K., Nakayama, T. *et al.* 2003. Role of Valpha 14 NKT cells in the development of impaired liver regeneration *in vivo*. *Hepatology.* 38:1116.
36 Kasahara, S., Ando, K., Saito, K. *et al.* 2003. Lack of tumor necrosis factor alpha induces impaired proliferation of hepatitis B virus-specific cytotoxic T lymphocytes. *J. Virol.* 77:2469.
37 Bachmann, M. F., Schorle, H., Kuhn, R. *et al.* 1995. Antiviral immune responses in mice deficient for both interleukin-2 and interleukin-4. *J. Virol.* 69:4842.
38 Widmer, M. B. and Grabstein, K. H. 1987. Regulation of cytolytic T-lymphocyte generation by B-cell stimulatory factor. *Nature.* 326:795.
39 Farrar, W. L., Johnson, H. M. and Farrar, J. J. 1981. Regulation of the production of immune interferon and cytotoxic T lymphocytes by interleukin 2. *J. Immunol.* 126:1120.
40 Hayakawa, Y., Takeda, K., Yagita, H., Van Kaer, L., Saiki, I. and Okumura, K. 2001. Differential regulation of Th1 and Th2 functions of NKT cells by CD28 and CD40 costimulatory pathways. *J. Immunol.* 166:6012.
41 Nishimura, T., Kitamura, H., Iwakabe, K. *et al.* 2000. The interface between innate and acquired immunity: glycolipid antigen presentation by CD1d-expressing dendritic cells to NKT cells induces the differentiation of antigen-specific cytotoxic T lymphocytes. *Int. Immunol.* 12:987.
42 Fujii, S., Liu, K., Smith, C., Bonito, A. J. and Steinman, R. M. 2004. The linkage of innate to adaptive immunity via maturing dendritic cells *in vivo* requires CD40 ligation in addition to antigen presentation and CD80/86 costimulation. *J. Exp. Med.* 199:1607.
43 Feau, S., Facchinetti, V., Granucci, F. *et al.* 005. Dendritic cell-derived IL-2 production is regulated by IL-15 in humans and in mice. *Blood.* 105:697.

Liver International ISSN 1478-3223

BASIC STUDIES

Upregulation of indoleamine 2,3-dioxygenase in hepatocyte during acute hepatitis caused by hepatitis B virus-specific cytotoxic T lymphocytes *in vivo*

Naoki Iwamoto[1], Hiroyasu Ito[1], Kazuki Ando[1], Tetsuya Ishikawa[2], Akira Hara[3], Ayako Taguchi[3], Kuniaki Saito[4], Masao Takemura[1], Michio Imawari[5], Hisataka Moriwaki[6] and Mitsuru Seishima[1]

1 Department of Informative Clinical Medicine, Gifu University Graduate School of Medicine, Gifu, Japan
2 Cancer Immunotherapy Center, Nagoya Kyoritsu Hospital, Nakagawa, Nagoya, Japan
3 Department of Tumor Pathology, Gifu University Graduate School of Medicine, Gifu, Japan
4 Human Health Sciences, Graduate School of Medicine and Faculty of Medicine, Kyoto University, Sakyo, Kyoto, Japan
5 Second Department of Internal Medicine, Showa University School of Medicine, Shinagawa-ku, Tokyo, Japan
6 First Department of Internal Medicine, Gifu University Graduate School of Medicine, Gifu, Japan

Keywords
cytotoxic T lymphocyte – hepatitis B virus – indoleamine 2,3-dioxygenase

Correspondence
Dr. Hiroyasu Ito, Department of Informative Clinical Medicine, Gifu University Graduate School of Medicine, 1-1 Yanagido, Gifu 501-1194, Japan
Tel: +81 58 230 6430
Fax: +81 58 230 6431
e-mail: hito@gifu-u.ac.jp

Received 16 January 2008
Accepted 27 February 2008

DOI:10.1111/j.1478-3231.2008.01748.x

Abstract

Background/Aims: Indoleamine-2,3-dioxygenase (IDO) is a tryptophan-catabolizing enzyme inducing suppression of T-cell function and immune tolerance. In hepatitis B virus (HBV) transgenic (Tg) mice, the adoptive transfer of HBV-specific cytotoxic T lymphocytes (CTL) causes a necroinflammatory liver disease that is histologically similar to acute viral hepatitis in man. The present study aimed to determine IDO expression in the liver and hepatocytes during an acute hepatitis model. *Methods:* Serum L-kynurenine (L-Kyn) concentration in HBV Tg mice administered with HBV-specific CTL was measured over time, together with serum levels of alanine aminotransferase (ALT). Furthermore, we examined the expression of IDO in the total liver and isolated hepatocytes of HBV Tg mice after CTL injection using immunohistochemical analysis and reverse-transcription polymerase chain reaction (PCR). *Results:* In HBV Tg mice, HBV-specific CTL induced, over the course of several days, a chronic increase in serum L-Kyn levels, which was associated with a sustained enhancement of liver IDO activity. In particular, IDO expression was enhanced in the liver parenchymal cells (hepatocytes) after HBV-specific CTL injection both in immunohistochemical analysis and in reverse-transcription PCR. Moreover, murine recombinant interferon-γ (IFN-γ) directly increased the IDO expression in primary hepatocytes *in vitro*. *Conclusions:* Cytotoxic T lymphocytes transduction results in the upregulation of IDO, which might downregulate T-cell responsiveness. Our findings provide evidence that hepatocyte itself expresses IDO and increases levels of L-Kyn in the blood in acute lethal hepatitis of mice. These data indicate that HBV infection facilitates the induction of IDO in response to proinflammatory cytokines, particularly IFN-γ.

Fulminant hepatitis is a clinical syndrome consisting of sudden and severe liver dysfunction that causes hepatic encephalopathy and acute liver dysfunction (1). Fulminant hepatitis develops in about 1% of patients with acute hepatitis B (2) and its mortality remains high. Hepatitis B virus (HBV) is a nonlytic virus that does not cause direct infected cell damage (3). Liver damage and viral clearance after HBV infection are thought to be mediated by the host cellular immune response to viral antigens. A fulminant hepatitis model has been created in mice by adoptive transfer of HBV-specific cytotoxic T lymphocytes (CTL) into HBV transgenic (Tg) mice. This liver injury consists of three steps after the CTL injection (4). The mice develop a necroinflammatory liver disease that is histologically similar to acute viral hepatitis in man.

Indoleamine 2,3-dioxygenase (IDO) is an enzyme, ubiquitously distributed in mammalian tissues and cells, converting L-tryptophan (L-Trp) to *N*-formylkynurenine, which is further catabolized to L-kynurenine (L-Kyn). IDO is induced by interferon-γ (IFN-γ)-dependent and/or an independent mechanism and other pro-inflammatory cytokines in the course of an inflammatory response in cell types including macrophages, fibroblasts and epithelial cells (5, 6). Increased IDO activity provokes tolerance of antigen-presenting cells and deprives T cells of L-Trp, leading to proliferation arrest and T-cell apoptosis (7, 8). On the other hand, L-Kyn has been shown to act as an immunoregulatory molecule that mediates immunosuppressive effects in the tissue microenvironment. IDO activity contributes to maternal tolerance in pregnancy (9), control of allograft rejection (10) and protection against autoimmunity (11). IDO has been found in various tumours of different histotypes and increments in IDO activity correlate with tumour progression (12). Therefore, the activity of IDO might play an important role in the regulation of the immune response exerted by the antigen-presenting cells and also might provide transformed cells with a potent tool to escape the immune system assault. Furthermore, IDO activity in white

blood cells and in different organs significantly increases in the course of viral, microbial, fungal or other parasite infections and it has been proposed that this enzyme is an important component in the overall defense mechanism (13–16).

The activity of IDO in acute hepatitis has been poorly understood and no studies have attempted to confirm the induction of IDO in hepatocytes *in vivo*. We examined herein whether IDO expression in hepatocytes is induced during acute liver injury caused by HBV-specific CTL using HBV Tg mice.

Materials and methods

Mice

Male B10.D2 (H-2d) mice (age, 6–8 weeks; weight, 25–30 g) were obtained from Japan SLC Inc. (Shizuoka, Japan). HBV-Tg mice lineage 107-5D (official designation Tg [Alb-1, HBV] Bri66), (inbred B10.D2, H-2d), in which the HBV envelope coding region is under the control of the mouse albumin promoter, were generously provided by Dr Francis V. Chisari, Department of Molecular and Experimental Medicine, Scripps Research Institute, La Jolla, CA, USA. All procedures were conducted in accordance with the National Institutes of Health Guide for the Care and Use of Laboratory Animals, and with the guidelines for care and use of animals established by the Animal Care and Use Committee of Gifu University.

Hepatitis B surface antigen-specific cytotoxic lymphocytes

Hepatitis B virus Tg mice were injected with a hepatitis B surface antigen (HBsAg)-specific, H-2d-restricted, $CD8^+$ CTL clone (designated 6C2) that recognizes an epitope (IPQSLDSWWTSL) located between residues 28 and 39 of HBsAg (4). At 5 days after the last stimulation, the cells were washed, counted and injected intravenously into HBV Tg mice.

Induction and assessment of liver cell injury

5×10^6 cells of the HBsAg-specific CTL clone 6C2 that we have previously shown (4) to induce severe Ag-dependent, major histocompatibility complex-class I-restricted liver cell injury in HBV envelope Tg mice were injected into the lateral tail vein in 200 µl of sterile saline. Before and at several time points, mice were bled by retro-orbital phlebotomy and the sera were analysed for the development of liver cell injury by measuring serum alanine aminotransferase activity (ALT). In selected experiments, hepatocellular injury and inflammation were confirmed by the examination of zinc formalin-fixed liver tissue sections stained with haematoxylin and eosin (HE).

Determination of L-kynurenine concentrations

Plasma from the mice was mixed with three volumes of 3% perchloric acid, and tissue samples were sonicated in four volumes of 3% perchloric acid. After centrifugation, the concentrations of L-Kyn in the supernatants were measured using high-performance liquid chromatography (HPLC) with a 5-mm octyldecyl silane column (150 mm by 2.1 mm; Eicom, Kyoto, Japan) and a spectrophotometric detector or a fluorescence spectrometric detector as described previously (17). UV signals were monitored at 355 nm for L-Kyn. The mobile phase consisted of 2.5% acetonitrile in 0.1 M sodium acetate (pH 3.9) and was filtered through a 0.45-µm-pore-size HA-type filter obtained from Millipore Corp. (Bedford, MA, USA). The flow rate was maintained at 0.75 ml/min throughout the chromatographic run.

Histopathological examination

Tissues were fixed in 10% formalin in phosphate-buffered saline overnight. Specimens were then embedded in paraffin. Three-micrometre sections were used for HE staining and IDO immunohistochemistry. For the immunohistochemistry, the deparaffinized sections were heated in 0.1 M citrate buffer (pH 6.0) using the Pascal® heat-induced target retrieval system (Dako, Carpinteria, CA, USA). Nonspecific antibody-binding sites were blocked in 0.01 M phosphate-buffered saline (PBS), pH 7.4, containing 2% bovine serum albumin (BSA; Wako, Osaka, Japan) for 60 min. Then the sections were incubated with rabbit anti-IDO polyclonal antibody (anti-mouse IDO antibody was generated by the peptide [H]-CMKPSKKKPTDGDKS-[OH]) 1:100 in 2% BSA/PBS and incubated overnight at 4 °C. Expression of the IDO protein was shown by the labelled streptavidin biotin (LSAB) method using the LSAB kit (Dako, Kyoto, Japan) containing biotinylated antibody and peroxidase-labelled streptavidin. The peroxidase-binding sites were detected by staining with 3,3′-diaminobenzidine. Finally, counterstaining was performed using Mayer's haematoxylin.

Isolation of mouse hepatocytes

The abdomen of a sacrificed mouse was opened and a needle was inserted into the vena cava. The portal vein was punctured. The liver was perfused with PBS and liver perfusion medium (Invitrogen Life Technologies, Carlsbad, CA, USA). To obtain nonparenchymal cell (NPC) populations, the liver was perfused with liver digestion medium (Invitrogen Life Technologies), removed and gently pressed through a mesh. NPC populations were separated from parenchymal hepatocytes by centrifugation at 50 *g* for 5 min (18). The purified cell population obtained in the final cell pellet was composed of ≥96% hepatocytes as previously reported (19, 20).

Quantification of indoleamine 2,3-dioxygenase mRNA by reverse-transcription and real-time polymersase chain reaction

Total RNA from tissues was rapidly isolated using an ISOGEN kit for RNA isolation (Nippon Gene, Tokyo, Japan). Total RNA (1 µg) was used for the synthesis of the first strand of cDNA. Reverse-transcription (RT)-polymerase chain reaction (PCR) was performed using an mRNA-selective PCR kit (Takara Biomedicals, Tokyo, Japan). The sample was reverse transcribed in a final volume of 50 µl at 50 °C for 30 min. The subsequent PCR was performed at 85 °C for 1 min, 55 °C for 1 min and 72 °C for 1 min. The final cycle was performed at 72 °C for 4 min. The nucleotide sequences for the forward and reverse primers for mouse IDO and β-actin were described previously (17). The final PCR products were electrophoresed on 2.5% agarose gels and visualized using UV light illumination after ethidium bromide staining. The resulting cDNA was used as a template for real-time PCR along with primer/probe sets for the IDO genes (TaqMan Gene Expression Assays; Applied Biosystems, Foster City, CA, USA) and 2 × Taqman universal PCR master mix (Applied Biosystems) according to the manufacturer's recommendations. Primer/probe sets for 18S were used as an internal control in each reaction (Applied Biosystems).

Real-time PCR data were analysed using sequence detector software (Applied Biosystems).

Culture of hepatocytes

Isolated hepatocytes were cultivated in Dulbecco's modified Eagle's medium supplemented with 10% foetal bovine serum and were maintained at 37 °C in a humidified atmosphere of 95% air and 5% CO_2 as described previously (21). After 24 h, the medium was replaced with fresh medium containing cytokine. At this time, the cells adhered to the bottom and the murine recombinant IFN-γ was added to induce IDO. The medium was replaced with 0 and 500 U/ml IFN-γ, and then incubated for an additional 24 h.

Data analysis

All data were expressed as means ± standard deviation (SD), and Student's *t*-test was used for the statistical analysis. Values were considered to be significantly different when the *P*-value was < 0.05.

Results

Hepatitis B virus-specific cytotoxic T lymphocytes induce an acutely fatal necroinflammatory liver disease (fulminant hepatitis) in Hepatitis B virus Tg Mice

Hepatitis B virus-specific $CD8^+$ CTL clone, designated 6C2, was used in this study because of its excellent cytotoxic and growth characteristics *in vitro*. Most studies were performed by the injection of clone 6C2 into lineage 107-5D. In this study, the severity of liver damage (evaluated by serum ALT levels) was greater in HBV Tg mice (6143 ± 1406 U/L) than in non-Tg littermate mice (39 ± 3 U/L) ($P < 0.001$) 24 h after administration of 5×10^6 CTL. Histological changes in the liver of HBV Tg mice were examined on days 0, 3 and 7 after HBV-specific CTL injection. A histological analysis revealed widely scattered necroinflammatory foci, containing mostly mononuclear cells and apoptotic hepatocytes in the liver after the CTL injection. On the other hand, non-Tg littermate mice were also examined histologically at the same time points after CTL injection. In non-Tg littermate mice, the invasion of a large amount of inflammatory cells and hepatocellular necrosis was not observed (data not shown).

Immunohistopathological examination on the expression of indoleamine 2,3-dioxygenase in the liver

Next, in order to verify IDO expression in the liver, we stained the liver tissues with anti-mouse IDO monoclonal antibody after HBV-specific CTL injection. Immunohistopathological examination revealed that IDO expression was upregulated in the hepatocytes of HBV Tg mice 7 days after HBV-specific CTL injection (Fig. 1E, F). In particular, the increase in IDO expression was observed in the liver parenchymal cells around the central vein. On the other hand, an increase in IDO expression in the liver could not be confirmed in non-Tg littermate mice after the CTL injection (Fig. 1I, J). Moreover, we measured the IDO expression in the hepatocytes of HBV Tg mice 1 and 3 days after HBV-specific CTL injection. The weak increase in IDO expression was also observed in the hepatocytes 1 and 3 days after CTL injection (Fig. 2).

Temporal profiles of indoleamine 2,3-dioxygenase induction in hepatitis B virus Tg mice injected with hepatitis B virus-specific cytotoxic T lymphocytes

We investigated the time course of changes in serum L-Kyn concentrations and mRNA expression in the liver of HBV Tg mice injected with HBV-specific CTL (Fig. 3 and Fig. 4A). Serum L-Kyn levels in HBV Tg mice were significantly increased at least as early as day 1 after CTL injection compared with non-Tg littermate mice (0.87 ± 0.28 versus 2.91 ± 0.92 μM; $P < 0.01$), and this increase in serum L-Kyn levels persisted on day 7 after CTL injection. The total liver IDO mRNA expression level in HBV Tg mice was increased on day 1 and day 3 after HBV-specific CTL injection (Fig. 4A). On the other hand, this enhancement of IDO expression was not observed in non-Tg littermate mice after CTL injection. Because immunohistopathological examination revealed that IDO expression was increased in the hepatocytes of HBV Tg mice after the CTL injection, we examined the IDO mRNA expression level in isolated hepatocytes alone from HBV Tg mice treated with CTL. The hepatocyte IDO mRNA expression level was markedly increased on day 1 after the CTL injection (Fig. 4B). Next, we measured IDO expression in the liver and hepatocytes by using the real-time PCR method (Fig. 4C). The increase of IDO expression in the hepatocytes of the HBV Tg mice was observed at 3 days after the CTL injection.

The effect of interferon-γ on indolamine 2,3-dioxygenase expression in hepatocytes

Indolamine 2,3-dioxygenase is believed to be induced by an IFN-γ-dependent and/or independent mechanism and IFN-γ is known to be highly enhanced in the liver of HBV Tg mice after HBV-specific CTL injection. Therefore, we examined the direct IFN-γ effect on primary hepatocytes *in vitro*. As shown in Figure 5, the IDO mRNA expression level in nontreated primary hepatocytes was not increased, but murine recombinant IFN-γ induced the IDO mRNA expression in both primary hepatocytes of HBV Tg and non-Tg littermate mice.

Discussion

In the present study, we have shown that the IDO expression in hepatocytes and serum L-Kyn concentration increased during the severe liver injury induced by HBV-specific CTL. This murine acute hepatitis model is thought to be similar to acute viral hepatitis in man (4). In the acute phase of this model, various cytokines, especially IFN-γ, are increased in the liver and many host inflammatory cells infiltrate the liver. Therefore, we speculated that IDO expression is enhanced during acute liver injury similar to acute viral hepatitis. Indeed, as shown in Figure 1, IDO expression in the liver of HBV Tg mice, in particular hepatocytes, was increased after HBV-specific CTL injection. Concurrently, an increase in serum L-Kyn concentration was observed during acute liver injury. In brief, this increase in the serum L-Kyn level can be explained by the enhancement of IDO expression in hepatocytes of HBV Tg mice administered CTL. The IDO mRNA expression in hepatocytes rapidly was enhanced after CTL injection and the enhancement was observed at 3 days after CTL injection (Fig. 4C). On the other hand, immunohistopathological examination revealed that IDO expression was slightly enhanced at 1 and 3 days after CTL injection and strongly enhanced at 7 days after CTL injection (Fig. 2). These data indicated that IDO

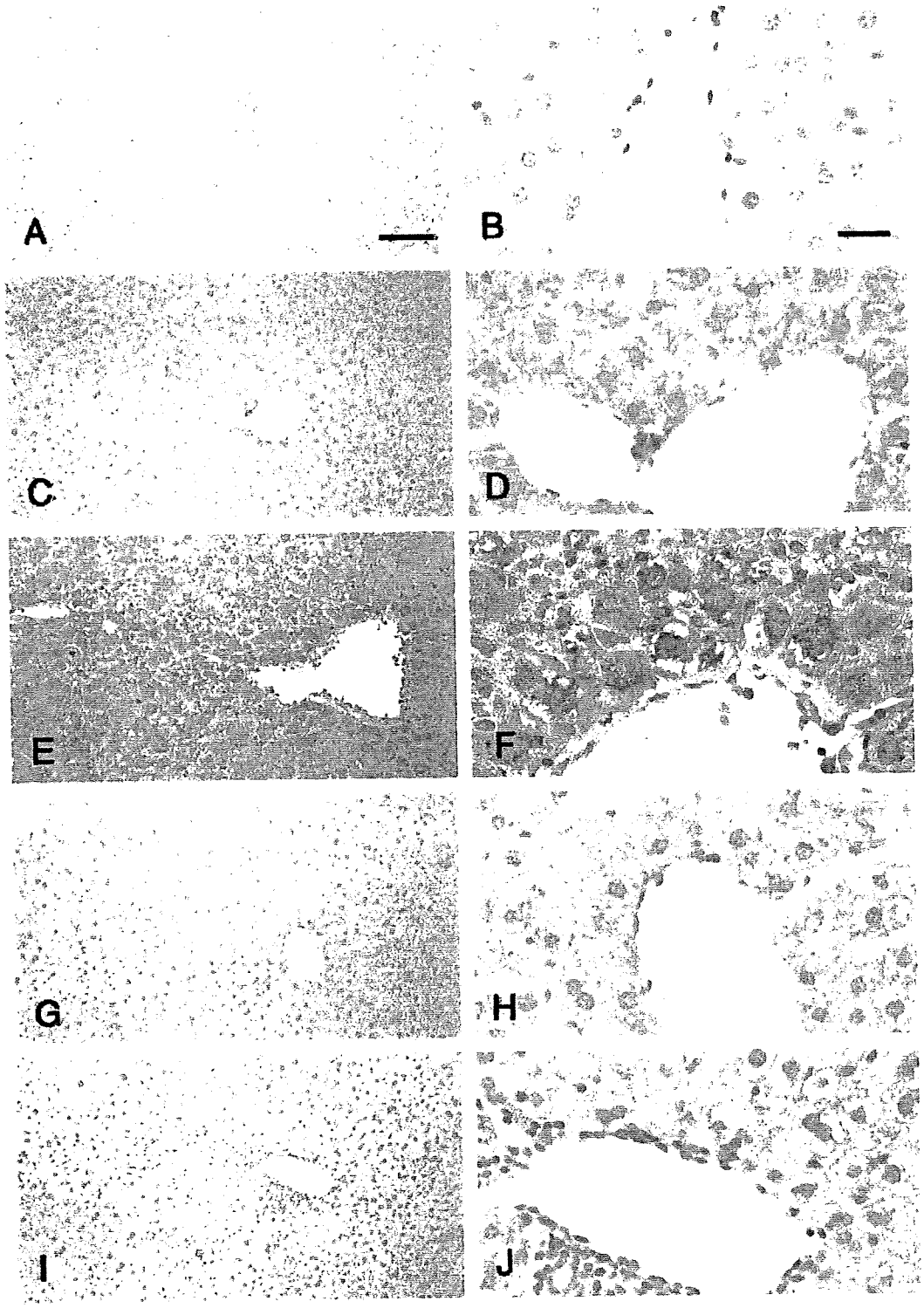

Liver International (2009)

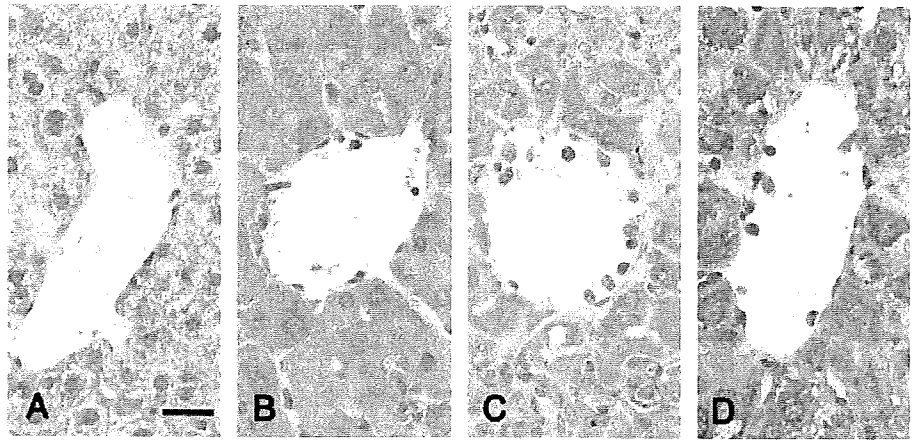

Fig. 2. Time-course of representative microphotographs of immunohistochemical staining for indole 2,3-dioxygenase in the liver tissues of a hepatitis B virus Tg mouse model on 0 (A), 1st (B), 3rd (C) and 7th (D) day after intravenous injection of cytotoxic T lymphocytes. Scale bar in panel A; 25 μm.

in hepatocytes may rapidly induce and stably exist for 7 days after CTL injection.

Most recently, it has been reported that IDO expression in the liver and serum kynurenine/tryptophan ratio in patients with chronic hepatitis C (HCV) were increased (15) and that this upregulation of IDO was caused by the IFN-γ produced by activated T cells in the liver with HCV. In the present study, we demonstrated that IDO expression in acute hepatitis is also enhanced, and confirmed that this enhancement was derived from hepatocytes. Therefore, it is likely that proinflammatory cytokine, such as IFN-γ, which is one of the inducing factor, is critical in the enhancement of IDO expression in hepatocytes during acute and chronic hepatitis.

The catabolism of L-Trp is differentially controlled during health and disease by two distinct enzymes: tryptophan 2,3-dioxygenase (TDO) and IDO. TDO is predominantly located in the liver and has a very strict substrate specificity, acting only on L-Trp (22), while IDO has a lower substrate specificity and is present in most mammalian cells including human mononuclear macrophages. Previous studies suggested that the activity of hepatocellular TDO decreased and IDO was induced in extrahepatic sites during inflammation and disease (23), resulting in the downregulation of L-Trp metabolism in the liver. However, our findings suggest that the IDO expression in hepatocytes was enhanced during acute hepatitis *in vivo*. As shown in Figure 5, the IDO expression in primary hepatocytes was induced by murine recombinant IFN-γ *in vitro*. In this acute hepatitis model, a large amount of IFN-γ is produced by HBV-specific CTL that directly contact HBsAg-positive hepatocytes (4, 24). Moreover, IFN-γ mRNA expression was upregulated at least 3–5 days after CTL injection in this murine acute hepatitis model (25). Therefore, it is assumed that the IDO expression in HBV Tg mice hepatocytes is enhanced in the early phase after HBV-specific CTL injection and the enhancement was sustained at 7 days after CTL injection. It was previously reported that bacterial lipopolysaccharide (LPS), a potent inducer of inflammatory cytokines *in vivo*, causes a severe acute liver disease in HBV Tg mice (26). We also examined the activity of IDO expression in hepatocytes when HBV Tg mice were administered LPS *in vivo*. The activity of IDO in hepatocytes was enhanced in LPS-induced liver injury just as in CTL-induced liver injury in HBV Tg mice (data not shown). It is thought that IFN-γ plays a critical role in these two models, and that the activity of IDO may be enhanced in IFN-γ-related liver injury.

Evidence accumulated over the last few years has indeed shown that the regulation of IDO expression and activity is an important event in the process leading to T lymphocyte proliferation and in the modulation of the immune responses (8, 27, 28). IDO activity contributes to maternal tolerance in pregnancy, control of allograft rejection, tumour progression and protection against autoimmunity (9, 29). In all these disorders, serum L-Trp concentrations are reduced while L-Kyn levels are elevated. Indeed, two major theories of L-Trp catabolism recently have been proposed to account for immune tolerance induction via L-Trp catabolism. One theory assumes that downstream metabolites of L-Trp catabolism, collectively known as L-Kyn, act to suppress immune reactivity, probably through direct interactions with effector T lymphocytes, natural killer (NK) cells and other cell types. The other theory posits that L-Trp itself has a key role and breakdown of this molecule suppresses T-cell proliferation by critically reducing

Fig. 1. Immunohistochemistry of indole 2,3-dioxygenase in the liver tissues of a hepatitis B virus (HBV) Tg mouse model on the seventh day after intravenous injection of cytotoxic T lymphocyte (CTL). (A, B) Liver tissue of negative control; (C, D) liver tissue before injection of CTL in HBV Tg mouse; (E, F) liver tissue 7 days after injection of CTL in HBV Tg mouse; (G, H) liver tissue before injection of CTL in non-Tg littermate mouse; (I, J) liver tissue 7 days after injection of CTL in non-Tg littermate mouse. A, C, E, G and I; low-power field of liver tissue, B, D, F, H and I; high-power field of view around the central vein. Scale bars in panel A; 100 μm and B; 25 μm. The severity of liver damage (evaluated by serum alanine transferase levels) was greater in HBV Tg mice (6143 ± 1406 U/L) than in non-Tg littermate mice (39 ± 3 U/L) ($P < 0.001$) 24 h after administration of 5×10^6 CTL.

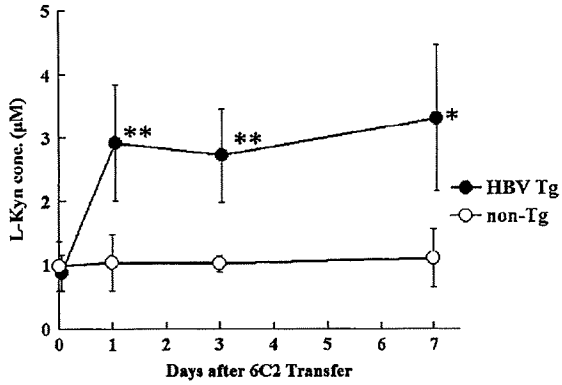

Fig. 3. High-performance liquid chromatography (HPLC) analysis of L-kynurenine (L-Kyn) concentrations in acute hepatitis of hepatitis B virus (HBV) Tg mice. L-Kyn concentrations in serum determined by HPLC method on HBV Tg mice after cytotoxic T lymphocytes injection. Significantly different from non-Tg, $^{*}P < 0.05$, $^{**}P < 0.01$.

the availability of the indispensable amino acid under local tissue microenvironments. Highly expressed IDO in hepatocytes during the early phase of fulminant hepatitis might enable the cells to initially avoid immune attack and then to reduce T-cell and/or NK-cell priming and the infiltration of effector inflammatory cells via local L-Trp depletion. In this study, the peculiarity of HBV Tg mice with CTL is that serum L-Trp level was constant regardless of high serum L-Kyn concentration and increased IDO activity in hepatocytes. Recently, it was reported that programmed cell death (PD)-1:PD-L1, a cell surface signaling molecule known to inhibit T-cell function, interactions did contribute to the suppression of IFN-γ production by HBV-specific CTLs (30). The enhancement of IDO expression in hepatocytes may also be one mechanism responsible for the suppression of IFN-γ production by HBV-specific CTLs in the liver. One way to address this issue in the future would be with an experimental model of acute hepatitis B in HBV Tg/IDO-knockout mice.

In conclusion, in liver injury caused by HBsAg-specific CTL in HBV Tg mice, IDO expression is increased in hepatocytes. These data indicate that HBV infection facilitates the induction of IDO in response to proinflammatory cytokines, particularly IFN-γ.

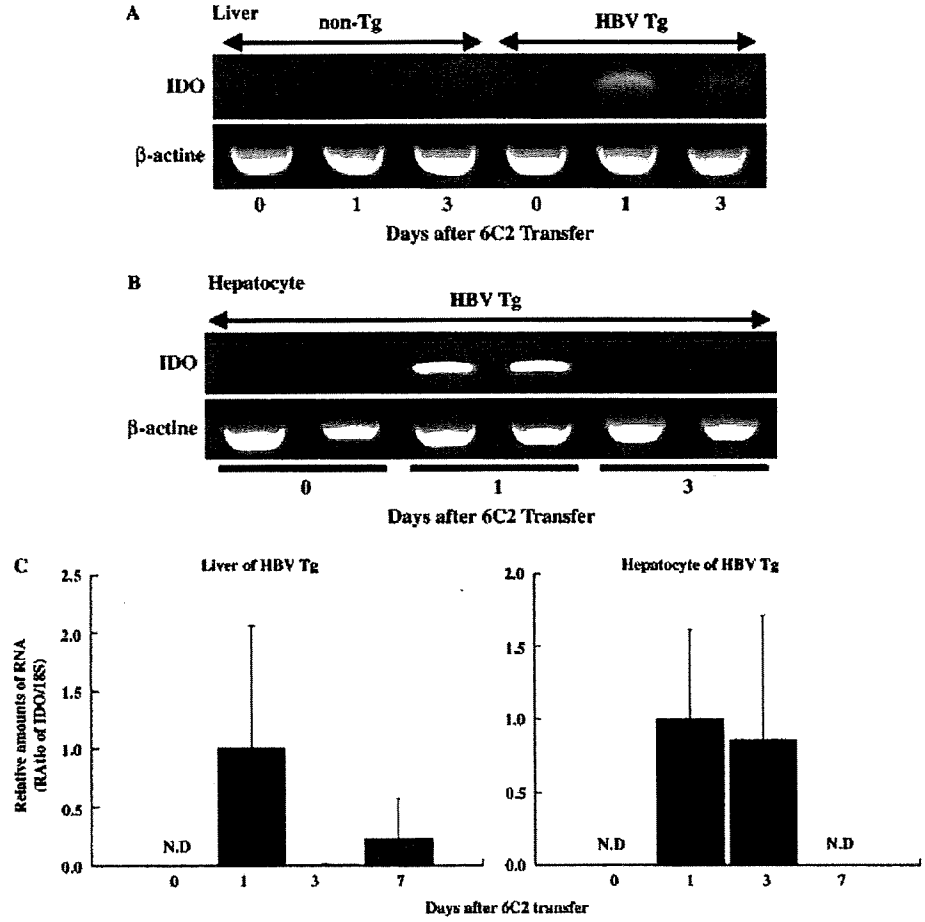

Fig. 4. Reverse-transcription (RT) polymerase chain reaction (PCR) analysis of indole 2,3-dioxygenase (IDO) mRNA expression in liver (A) and hepatocyte (B). Hepatitis B virus (HBV) Tg mice were injected with cytotoxic T lymphocytes (CTL). IDO mRNA levels were measured using RT-PCR. β-actin is shown as a loading control. PCR for β-actin was performed with the same cDNA samples. The relative expression levels of IDO mRNA in livers and hepatocytes on HBV Tg mice injected with CTL were measured using quantitative real-time PCR. Results were normalized by the expression of 18S mRNA (C). N. D.; not detected.

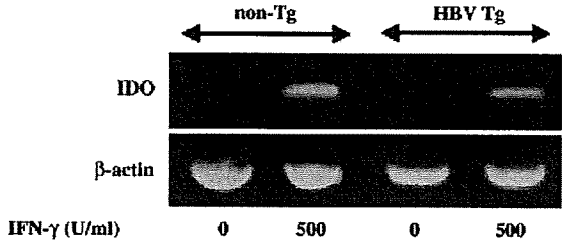

Fig. 5. Reverse-transcription polymerase chain reaction (PCR) analysis of indole 2,3-dioxygenase (IDO) mRNA expression in primary cultured hepatocytes from mice. Hepatocytes were cultivated in Dulbecco's modified Eagle's medium supplemented with 10% foetal bovine serum and maintained at 37 °C in a humidified atmosphere of 95% air and 5% CO_2. Hepatocytes were obtained from non-Tg littermate mice. After 24 h, the medium was replaced with fresh medium containing cytokine. At this time, the cells adhered to the bottom and interferon-γ (IFN-γ) was added to induce IDO. The medium was replaced with 0 and 500 U/ml IFN-γ, and then incubated for an additional 24 h.

Acknowledgements

We thank Francis V. Chisari (The Scrips Research Institute) for providing the HBV transgenic mice and an HBsAg-specific $CD8^+$ CTL clone (designated 6C2). We express our gratitude to John Cole for reading our draft and giving us suggestions on language and style.

References

1. Wright TL, Lau JY. Clinical aspects of hepatitis B virus infection. *Lancet* 1993; **342**: 1340–4.
2. Lettau LA, McCarthy JG, Smith MH, *et al.* Outbreak of severe hepatitis due to delta and hepatitis B viruses in parenteral drug abusers and their contacts. *N Engl J Med* 1987; **317**: 1256–62.
3. Chisari FV, Ferrari C. Hepatitis B virus immunopathology. *Springer Semin Immunopathol* 1995; **17**: 261–81.
4. Ando K, Moriyama T, Guidotti LG, *et al.* Mechanisms of class I restricted immunopathology, a transgenic mouse model of fulminant hepatitis. *J Exp Med* 1993; **178**: 1541–54.
5. Fujigaki S, Saito K, Sekikawa K, *et al.* Lipopolysaccharide induction of indoleamine 2,3-dioxygenase is mediated dominantly by an IFN-gamma-independent mechanism. *Eur J Immunol* 2001; **31**: 2313–8.
6. Murray HW, Szuro-Sudol A, Wellner D, *et al.* Role of tryptophan degradation in respiratory burst-independent antimicrobial activity of gamma interferon-stimulated human macrophages. *Infect Immun* 1989; **57**: 845–9.
7. Mellor AL, Munn DH. Tryptophan catabolism and T-cell tolerance: immunosuppression by starvation? *Immunol Today* 1999; **20**: 469–73.
8. Munn DH, Shafizadeh E, Attwood JT, Bondarev I, Pashine A, Mellor AL. Inhibition of T cell proliferation by macrophage tryptophan catabolism. *J Exp Med* 1999; **189**: 1363–72.
9. Mellor AL, Sivakumar J, Chandler P, *et al.* Prevention of T cell-driven complement activation and inflammation by tryptophan catabolism during pregnancy. *Nat Immunol* 2001; **2**: 64–8.
10. Grohmann U, Orabona C, Fallarino F, *et al.* CTLA-4-Ig regulates tryptophan catabolism *in vivo*. *Nat Immunol* 2002; **3**: 1097–101.
11. Grohmann U, Fallarino F, Bianchi R, *et al.* A defect in tryptophan catabolism impairs tolerance in nonobese diabetic mice. *J Exp Med* 2003; **198**: 153–60.
12. Huang A, Fuchs D, Widner B, Glover C, Henderson DC, Allen-Mersh TG. Serum tryptophan decrease correlates with immune activation and impaired quality of life in colorectal cancer. *Br J Cancer* 2002; **86**: 1691–6.
13. Fuchs D, Moller AA, Reibnegger G, Stockle E, Werner ER, Wachter H. Decreased serum tryptophan in patients with HIV-1 infection correlates with increased serum neopterin and with neurologic/psychiatric symptoms. *J Acquir Immune Defic Syndr* 1990; **3**: 873–6.
14. Yoshida R, Urade Y, Tokuda M, Hayaishi O. Induction of indoleamine 2,3-dioxygenase in mouse lung during virus infection. *Proc Natl Acad Sci USA* 1979; **76**: 4084–6.
15. Larrea E, Riezu-Boj JI, Gil-Guerrero L, *et al.* Upregulation of indoleamine 2,3-dioxygenase in hepatitis C virus infection. *J Virol* 2007; **81**: 3662–6.
16. Hissong BD, Byrne GI, Padilla ML, Carlin JM. Upregulation of interferon-induced indoleamine 2,3-dioxygenase in human macrophage cultures by lipopolysaccharide, muramyl tripeptide, and interleukin-1. *Cell Immunol* 1995; **160**: 264–9.
17. Fujigaki S, Saito K, Takemura M, *et al.* L-tryptophan-L-kynurenine pathway metabolism accelerated by *Toxoplasma gondii* infection is abolished in gamma interferon-gene-deficient mice: cross-regulation between inducible nitric oxide synthase and indoleamine-2, 3-dioxygenase. *Infect Immun* 2002; **70**: 779–86.
18. Ito H, Ando K, Nakayama T, *et al.* Role of V alpha 14 NKT cells in the development of impaired liver regeneration *in vivo*. *Hepatology* 2003; **38**: 1116–24.
19. Gregory SH, Wing EJ. IFN-gamma inhibits the replication of *Listeria monocytogenes* in hepatocytes. *J Immunol* 1993; **151**: 1401–9.
20. Gregory SH, Barczynski LK, Wing EJ. Effector function of hepatocytes and Kupffer cells in the resolution of systemic bacterial infections. *J Leukoc Biol* 1992; **51**: 421–4.
21. Heyes MP, Chen CY, Major EO, Saito K. Different kynurenine pathway enzymes limit quinolinic acid formation by various human cell types. *Biochem J* 1997; **326**(Pt 2): 351–6.
22. Schutz G, Beato M, Feigelson P. Messenger RNA for hepatic tryptophan oxygenase: its partial purification, its translation in a heterologous cell-free system, and its control by glucocorticoid hormones. *Proc Natl Acad Sci USA* 1973; **70**: 1218–21.
23. Takikawa O, Yoshida R, Kido R, Hayaishi O. Tryptophan degradation in mice initiated by indoleamine 2,3-dioxygenase. *J Biol Chem* 1986; **261**: 3648–53.
24. Yamasaki T, Handa H, Yamashita J, Watanabe Y, Namba Y, Hanaoka M. Specific adoptive immunotherapy of malignant glioma with long-term cytotoxic T lymphocyte line expanded in T-cell growth factor. Experimental study and future prospects. *Neurosurg Rev* 1984; **7**: 37–54.
25. Kakimi K, Lane TE, Wieland S, *et al.* Blocking chemokine responsive to gamma-2/interferon (IFN)-gamma inducible protein and monokine induced by IFN-gamma activity *in vivo* reduces the pathogenetic but not the antiviral potential of hepatitis B virus-specific cytotoxic T lymphocytes. *J Exp Med* 2001; **194**: 1755–66.
26. Gilles PN, Guerrette DL, Ulevitch RJ, Schreiber RD, Chisari FV. HBsAg retention sensitizes the hepatocyte to injury by physiological concentrations of interferon-gamma. *Hepatology* 1992; **16**: 655–63.
27. Frumento G, Rotondo R, Tonetti M, Damonte G, Benatti U, Ferrara GB. Tryptophan-derived catabolites are responsible for inhibition of T and natural killer cell proliferation induced by indoleamine 2,3-dioxygenase. *J Exp Med* 2002; **196**: 459–68.
28. Lee GK, Park HJ, Macleod M, Chandler P, Munn DH, Mellor AL. Tryptophan deprivation sensitizes activated T cells to apoptosis prior to cell division. *Immunology* 2002; **107**: 452–60.
29. Munn DH, Zhou M, Attwood JT, *et al.* Prevention of allogeneic fetal rejection by tryptophan catabolism. *Science* 1998; **281**: 1191–3.
30. Isogawa M, Furuichi Y, Chisari FV. Oscillating CD8 (+) T cell effector functions after antigen recognition in the liver. *Immunity* 2005; **23**: 53–63.

GASTROENTEROLOGY 2008;134:1396–1405

Potential Relevance of Cytoplasmic Viral Sensors and Related Regulators Involving Innate Immunity in Antiviral Response

YASUHIRO ASAHINA,* NAMIKI IZUMI,* ITSUKO HIRAYAMA,* TOMOHIRO TANAKA,* MITSUAKI SATO,*,‡ YUTAKA YASUI,* NOBUTOSHI KOMATSU,*,‡ NAOKI UMEDA,* TAKANORI HOSOKAWA,* KEN UEDA,* KAORU TSUCHIYA,* HIROYUKI NAKANISHI,* JUN ITAKURA,* MASAYUKI KUROSAKI,* NOBUYUKI ENOMOTO,‡ MEGUMI TASAKA,§ NAOYA SAKAMOTO,§ and SHOZO MIYAKE*

*Department of Gastroenterology and Hepatology, Musashino Red Cross Hospital, Tokyo; ‡First Department of Internal Medicine, Faculty of Medicine, University of Yamanashi, Yamanashi; and §Department of Gastroenterology and Hepatology, Tokyo Medical and Dental University, Tokyo, Japan

Background & Aims: **Clinical significance of molecules involving innate immunity in treatment response remains unclear. The aim is to elucidate the mechanisms underlying resistance to antiviral therapy and predictive usefulness of gene quantification in chronic hepatitis C (CH-C).** ***Methods:*** **We conducted a human study in 74 CH-C patients treated with pegylated interferon α-2b and ribavirin and 5 nonviral control patients. Expression of viral sensors, adaptor molecule, related ubiquitin E3-ligase, and modulators were quantified.** ***Results:*** **Hepatic RIG-I, MDA5, LGP2, ISG15, and USP18 in CH-C patients were up-regulated at 2- to 8-fold compared with non-hepatitis C virus patients with a relatively constitutive Cardif. Hepatic RIG-I, MDA5, and LGP2 were significantly up-regulated in nonvirologic responders (NVR) compared with transient (TR) or sustained virologic responders (SVR). Cardif and RNF125 were negatively correlated with RIG-I and significantly suppressed in NVR. Differences among clinical responses in RIG-I/Cardif and RIG-I/RNF125 ratios were conspicuous (NVR/TR/SVR = 1.3:0.6:0.4 and 2.3:1.3:0.8, respectively). Like viral sensors, ISG15 and USP18 were significantly up-regulated in NVR (4-fold and 2.3-fold, respectively). Multivariate and receiver operator characteristic analyses revealed higher RIG-I/Cardif ratio, ISG15, and USP18 predicted NVR. Lower Cardif in NVR was confirmed by its protein level in Western blot. Also, transcriptional responses in peripheral blood mononuclear cells to the therapy were rapid and strong except for Cardif in not only a positive (RIG-I, ISG15, and USP18) but also in a negative regulatory manner (RNF125).** ***Conclusions:*** **NVR may have adopted a different equilibrium in their innate immune response. High RIG-I/Cardif and RIG-I/RNF125 ratios and ISG15 and USP18 are useful in identifying NVR.**

Infection with hepatitis C virus (HCV) is a common cause of chronic hepatitis, which progresses to cirrhosis and hepatocellular carcinoma in many patients.[1] Although combination therapy with pegylated interferon (PEG-IFN) α and ribavirin is now established as the standard treatment for chronic HCV infection genotype 1b, the sustained virologic response rate in these patients is still around 50%.[2–4] Moreover, physicians have also found that 20% of patients are nonvirologic responders (NVR; those whose HCV-RNA does not become negative during 48 weeks of combination therapy).[5] Prediction of NVR status is of clinical importance because these patients have no chance of achieving a sustained virologic response even after prolonged combination therapy.[6] However, mechanisms involving resistance to PEG-IFN-α and ribavirin have not been fully elucidated, and it is difficult to predict treatment responses before initiation of PEG-IFN-α and ribavirin combination therapy.

In vitro studies have suggested that an innate immune response in viral infection is an essential part of the host antiviral defense system.[7] HCV evades the host immune response through a complex combination of processes that include signaling interference, effector modulation, and continual viral genetic variation.[8] We hypothesized that liver tissue would show a consistent difference between responders and nonresponders in expression levels of the gene involved in innate immunity and IFN signal transduction. These differences could be used to predict treatment outcomes.

The retinoic acid–inducible gene I (RIG-I), a cytoplasmic RNA helicase, and the related melanoma differentia-

Abbreviations used in this paper: CARD, Caspase-recruiting domain; Cardif, caspase-recruiting domain adaptor inducing IFN-β; G3PDH, glyceraldehyde-3-phosphate dehydrogenase; HCV, hepatitis C virus; IPS-1, IFN-β promoter stimulator I; ISG15, IFN-stimulated gene 15; PEG-IFN, pegylated interferon; MDA5, melanoma differentiation associated gene 5; MAVS, mitochondrial antiviral signaling protein; NVR, nonvirologic responders; PBMC, peripheral blood mononuclear cell; RIG-I, retinoic acid-inducible gene I; RNF125, ring-finger protein 125; ROC, receiver operator characteristic; SVR, sustained viral responder; TR, transient responder; UBP43, ubiquitin-specific protease 43; USP18, ubiquitin-specific protease 18; VISA, virus-induced signaling adaptor.

0016-5085/08/$34.00
doi:10.1053/j.gastro.2008.02.019

Table 1. Patient Characteristics at Baseline According to Final Virologic Response

	SVR n = 30	TR n = 24	NVR n = 20	*P* value
Age (*y*)	52 ± 13	60 ± 8.7	60 ± 10	.04[a]
Female % (M/F)	47% (16/14)	63% (9/15)	60% (8/12)	.5[b]
Naïve & Relapser[c]/Non-responder[c]	26/4	20/4	14/6	.3[b]
BMI	24.6 ± 3.0	24.9 ± 4.4	24.0 ± 2.1	.6[a]
ALT (*IU/L*)	75 ± 57	65 ± 35	68 ± 41	1.0[a]
Hemoglobin (*g/dL*)	14.3 ± 1.6	14.1 ± 1.1	14.5 ± 1.7	.6[a]
Platelet count ($\times 10^3/\mu L$)	182 ± 62	169 ± 48	140 ± 39	.04[a]
Liver histology				
A1/A2/A3	19/8/3	14/8/1	10/10/0	.3[b]
F1/F2/F3	14/9/7	11/7/5	7/5/8	.7[b]
Viral load ($\times 10^6$ *IU/mL*)	1.6 ± 1.2	1.8 ± 1.1	1.6 ± 1.1	.8[a]
Viral decline rate (log_{10}/day)				
First phase	2.1 ± 0.9	1.5 ± 0.6	0.7 ± 0.5	<.0001[a]
Second phase	0.05 ± 0.05	0.04 ± 0.02	0.006 ± 0.008	<.0001[a]

ALT, alanine aminotransferase; BMI, body mass index.
[a]*P* values were determined by Kruskal–Wallis test.
[b]*P* values were determined by chi-square test.
[c]Response to previous IFN treatment.

tion-associated gene 5 (MDA5) play essential roles in initiating the host antiviral response by detecting intracellular viral dsRNA.[9,10] Caspase-recruiting domain (CARD) adaptor inducing IFN-β (Cardif), also called IFN-β promoter stimulator 1 (IPS-1), mitochondrial antiviral signaling protein (MAVS), and virus-induced signaling adaptor (VISA), is an adaptor molecule. Cardif connects RIG-I sensing to downstream signaling, resulting in IFN-β gene activation.[11–14] On the other hand, RIG-I sensing has been shown to be negatively regulated in a dominant-negative manner by LGP2,[10,15] a helicase related to RIG-I and MDA5 lacking CARD. Interestingly, the ubiquitin ligase ring-finger protein 125 (RNF125) has been recently shown to conjugate ubiquitin to RIG-I, MDA5 as well as Cardif, which results in suppressing the functions of these proteins.[16] Furthermore, these molecules are conjugated (ISGylated) by IFN-stimulated gene 15 (ISG15), a ubiquitin-like protein,[17] and ISG15 is specifically removed from ISGylated protein by ubiquitin-specific protease 18 (USP18), also called ubiquitin-specific protease 43 (UBP43).[18,19] Moreover, the NS3/4A protease of HCV specifically cleaves Cardif as part of its immune evasion strategy.[11,20] Therefore, the RIG-I/Cardif system and its regulatory systems have essential key functions in the innate antiviral response (see Supplementary Figure 1 online at www.gastrojournal.org). However, the clinical significance of these innate immune systems, especially in relevance to the treatment response, is unclear because findings in this field have been mainly obtained by in vitro experiments using cell lines.

The aims of this study were to elucidate the mechanisms underlying resistance to antiviral therapy in the clinical setting and to determine whether quantification of transcripts of positive and negative cytoplasmic viral sensors and related regulatory molecules involving innate immune system is useful in predicting responses to PEG-IFN-α and ribavirin combination therapy.

Patients and Methods

Patients

Among patients with biopsy-proven chronic hepatitis C hospitalized at the Musashino Red Cross Hospital, 74 patients of HCV genotype 1b with a high viral load (>100,000 IU/mL by Amplicor-HCV Monitor Assay; Roche Molecular Diagnostics Co, Tokyo, Japan) were included in the present study (Table 1). Patients with cirrhosis, autoimmune hepatitis, or alcoholic liver injury were excluded. No patient was positive for hepatitis B virus–associated antigen/antibody or anti–human immunodeficiency virus antibody. No patient received immunomodulatory therapy prior to the enrollment. Written informed consent was obtained from all the patients, and this study was approved by the Ethical Committee of Musashino Red Cross Hospital in accordance with the Helsinki Declaration. Five patients with nonviral liver disease (2 had autoimmune hepatitis and 3 had primary biliary cirrhosis) were included in the present study as controls.

Treatment Protocol

The patients were treated for 48 weeks with subcutaneous injections of PEG-IFN-α-2b (PegIntron; Schering-Plough Corporation, Kenilworth, NJ) at a dose of 1.5 $\mu g \cdot kg^{-1} \cdot week^{-1}$. Ribavirin (Rebetol; Schering-Plough Corporation) was administered concomitantly over the 48-week period, given orally twice daily at a total daily dose of 600 mg for the patients who weighed less than 60 kg and 800 mg for the patients who weighed between 60 and 80 kg. The dose of PEG-IFN-α-2b was reduced to 0.75 $\mu g \cdot kg^{-1} \cdot week^{-1}$ when either the neutrophil count was $<750/mm^3$ or the platelet count was $<80 \times 10^3/mm^3$. The dose of ribavirin was reduced to 600 mg/day when the hemoglobin concentration decreased to <10 g/dL.

Measurement of Gene Expression in the Liver

Liver biopsy was performed immediately before starting the therapy. After extraction of total RNA from liver biopsy specimens, the messenger RNA (mRNA) expression of positive and negative cytoplasmic viral sensors (RIG-I, MDA5, and LGP2), the adaptor molecule (Cardif), related ubiquitin E3-ligase (RNF125), and the modulators of these molecules (ISG15 and USP18) was quantified by real-time quantitative polymerase chain reaction (PCR) using primers specific for target genes. In brief, total RNA was extracted by the acid-guanidinium-phenol-chloroform method using Isogen (Nippon Gene Co Ltd, Toyama, Japan) from the liver biopsy specimen, which was 0.2–0.4 cm in length and 13 gauge in diameter. Complementary DNA (cDNA) was transcribed from 2 μg total RNA template in a 140-μL reaction mixture using a SYBR RT-PCR Kit (Takara Bio Co Ltd, Otsu, Japan) with random hexamer. Real-time quantitative PCR was performed using Smart Cycler version II (Takara Bio Co Ltd) with the SYBR RT-PCR Kit (Takara Bio Co Ltd) according to the manufacturer's instructions, and intercalating SYBR Green I (Molecular Probes Inc, Eugene, Oregon) was detected. Assays were performed in duplicate, and the expression levels of target genes were normalized to expression of the glyceraldehyde-3-phosphate dehydrogenase (G3PDH) gene and hydroxymethylbilane synthase, which is stable in the liver, as quantified using real-time quantitative PCR as internal controls. For accurate normalization, a set of 2 housekeeping genes was used in the present study. Sequences of primer sets were as follows: RIG-I: 5′-AAAGCATGCATGGTGTTCCAGA-3′, 5′-TCATTCGTGCATGCTCACTGATAA-3′; MDA5: 5′-ACATAACAGCAACATGGGCAGTG-3′, 5′-TTTGGTAAGGCCTGAGCTGGAG-3′; LGP2: 5′-ACAGCCTTGCAAACAGTACAACCTC-3′, 5′-GTCCCAAATTTCCGGCTCAAC-3′; Cardif: 5′-GGTGCCATCCAAAGTGCCTACTA-3′, 5′-CAGCACGCCAGGCTTACTCA-3′; RNF125: 5′-AGGGCACATATTCGGACTTGTCA-3′, 5′-CGGGTATTAAACGGCAAAGTGG-3′; ISG15: 5′-AGCGAACTCATCTTTGCCAGTACA-3′, 5′-CAGCTCTGACACCGACATGGA-3′; USP18: 5′-TGGTTCTGCTTCAATGACTCCAATA-3′, 5′-TTTGGGCATTTCCATTAGCACTC-3′; GAPDH: 5′-GCACCGTCAAGGCTGAGAAC-3′, 5′-TGGTGGTGAAGACGCCAGT-3′. hydroxymethylbilane synthase: 5′-AAGCGGAGCCATGTCTGGTAAC-3′, 5′-GTACCCACGCGAATCACTCTCA-3′.

Sequential Measurement of Gene Expression in Peripheral Blood Mononuclear Cells Before and During Therapy

To understand transcriptional response of the genes to PEG-IFN-α-2b and ribavirin therapy, serial expression of RIG-I, RNF125, Cardif, ISG15, and USP18 were determined before and during treatment in peripheral blood mononuclear cells (PBMC) in 14 patients (7 were sustained viral responders [SVR] and 7 were NVR). PBMC was obtained from whole blood samples collected before and at 4, 8, 24, 48, and 168 hours after the initiation of PEG-IFN-α-2b and ribavirin combination therapy. After extraction of total RNA from the PBMC, the expression of mRNA was quantified at each specified time point using real-time quantitative PCR as described above. Gene expression levels at each time point during treatment were calculated relative to baseline expression levels measured prior to IFN treatment.

Western Blotting

Western blotting was carried out in 9 patients (5 were SVR and 4 were NVR) and 3 non-HCV control subjects as described previously.[21] Liver biopsy specimen of ~10 mg was homogenized in 100 μL Complete Lysis-M (Roche Applied Science, Penzberg, Germany). Twenty micrograms of the homogenates were separated by SDS-PAGE and blotted onto a polyvinylidene difluoride Western blotting membrane. The membrane was incubated with the primary antibodies followed by a peroxidase-labeled anti-IgG antibody and visualized by chemiluminescence using the ECL Western blotting Analysis System (Amersham Biosciences, Buckinghamshire, United Kingdom). The anti-VISA mouse monoclonal antibody (BioDesign, Saco, ME) and anti-β-actin antibody (Sigma Chemical Co, St. Louis, MO) were used.

HCV Dynamics in Serum

To analyze the viral dynamics, HCV RNA was quantified just before and at 4, 8, and 24 hours and 2, 7, 14, 28, 56, and 84 days after the initiation of PEG-IFN-α-2b and ribavirin combination therapy, using real-time detection PCR, as reported previously.[22] For each patient, the viral decline curve was plotted on a semilogarithmic scale, and the slopes of the exponential viral declines were calculated for each viral decline phase with a straight-line fit of the data.

Definitions of Response to Therapy

A patient negative for serum HCV RNA during the first 6 months after the completion of PEG-IFN-α-2b and ribavirin combination therapy was defined as an SVR, and a patient for whom HCV RNA became negative at the end of therapy and reappeared after completion of therapy was defined as a transient responder (TR). A patient who was positive for HCV RNA even during the course of therapy was defined as an NVR. HCV RNA was determined with the Amplicor qualitative assay (Roche Molecular Diagnostics Co, Tokyo, Japan). The detection sensitivity of this assay is approximately 50 IU/mL.

Statistical Analysis

Categorical data were compared by the χ^2 test and Fisher exact test. Distributions of continuous variables were analyzed by Mann–Whitney U test for 2 groups. Kruskal–Wallis test was used for multiple group comparisons. All tests of significance were 2-tailed, and P values $< .05$ were considered statistically significant.

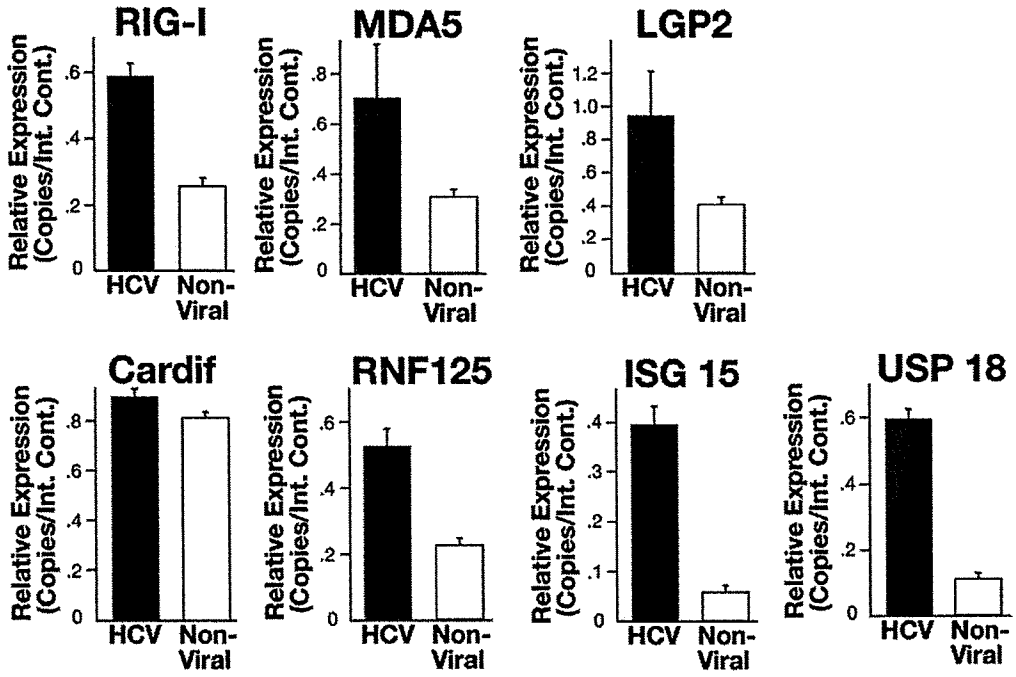

Figure 1. Comparison of hepatic gene expression levels between chronic hepatitis C patients (n = 74) and nonviral liver disease patients (n = 5). Expression levels of RIG-I, MDA5, LGP2, Cardif, RNF125, ISG15, and USP18 are shown. *Error bars* indicate the standard error. Upon HCV infection, expression of these genes except Cardif was stimulated. The *P* values determined by Mann–Whitney *U* test between 2 groups were as follows: RIG-I, *P* .02; MDA5, *P* .01; LGP2, *P* .005; Cardif, *P* .7; RNF125, *P* .06; ISG15, *P* .007; USP18, *P* .004.

Results

Patient Characteristics

According to the final virologic response, patients were classified into 3 groups: 30 were SVR, 24 were TR, and the remaining 20 were NVR, as shown in Table 1. Viral decline rates in NVR were significantly lower in both the first and second phases of HCV dynamics. It should be noted that most NVR patients exhibited no second-phase viral decline.

Data on factors that were available before starting the treatment were compared according to virologic response by univariate analysis. As shown in Table 1, only age and platelet count were associated with viral response, and no other clinical factors were predictive of NVR before initiation of the therapy.

Gene Expression Involving Innate Immunity in the Liver

First, we compared basal hepatic gene expression between the chronic hepatitis C patients (n = 74) and the nonviral liver disease patients (n = 5). As shown in Figure 1, levels of RIG-I, MDA5, LGP2, ISG15, and USP18 expression were significantly higher in the chronic hepatitis C patients than in the nonviral liver disease patients. However, there was no significant difference in levels of Cardif expression between the chronic hepatitis C and nonviral-related liver disease patients.

Next, to assess the relationship between baseline hepatic gene expression and treatment efficacy, levels of gene expression were compared based on the final virologic response. As shown in Figure 2, the hepatic expression levels of RIG-I, MDA5, and LGP2 were significantly higher in NVR than in SVR and TR. In marked contrast, hepatic Cardif expression was significantly lower in the NVR group. The hepatic expression of RNF125, which is specific E3-ubiquitin ligase for RIG-I, MDA5, and Cardif, was also significantly lower in the NVR group. Because negative correlation was found between RIG-I and Cardif or RNF125 expression, we calculated the ratio of RIG-I to Cardif or RNF125 expression levels. As shown in Figure 2, the difference among the groups was conspicuous when comparison was made with the RIG-I/Cardif ratio or RIG-I/RNF125 ratio. Moreover, the RIG-I/Cardif expression ratio before treatment was negatively and significantly correlated with the exponential viral decline rate in both the first and the second phases of HCV dynamics (first phase, $r = -0.4$, $P < .0005$; second phase, $r = -0.5$, $P < .0001$). Similar correlation was found between RIG-I/RNF125 ratio and viral decline rate (first phase, $r = -0.4$, $P = .004$; second phase, $r = -0.2$, $P = .09$, data not shown).

Like RIG-I and MDA5, intrahepatic expression levels of ISG15 and USP18 were significantly higher in NVR than in SVR and TR (Figure 2). When we assessed the correlation of these 2 genes in individual patients, we found a strong and significant correlation between ISG15 and USP18 ($r^2 = 0.88$, $P < .0001$). Levels of ISG15 and USP18 expression before treatment were negatively correlated with the exponential viral decline rates calculated from

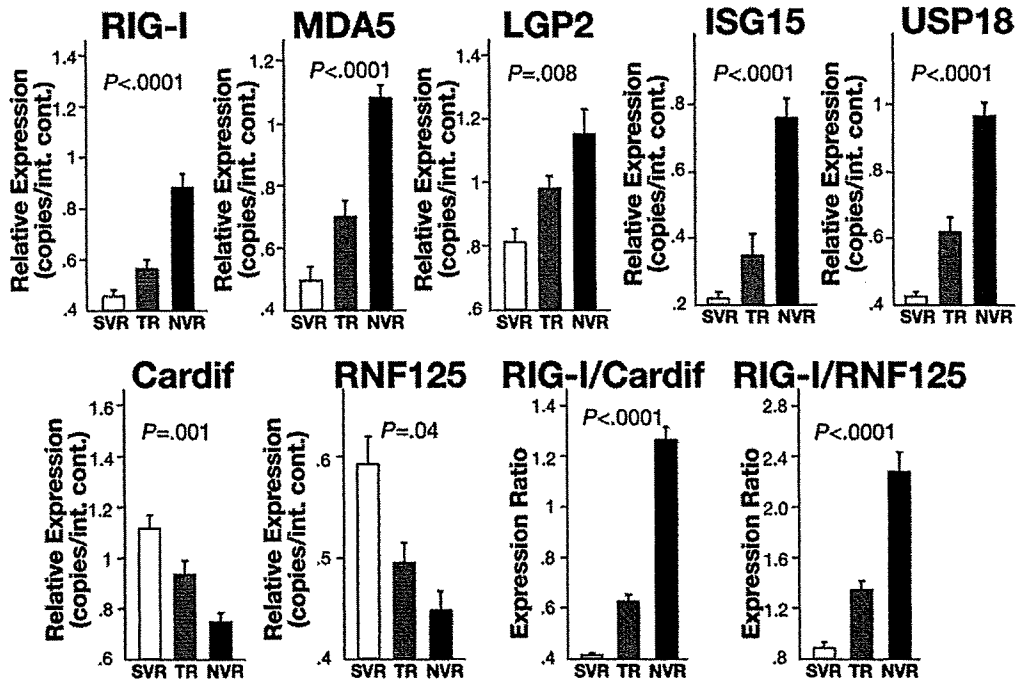

Figure 2. Comparison of hepatic gene expression levels according to final virologic outcome. Expression levels of RIG-I, MDA5, LGP2, ISG15, USP18, Cardif, RNF125, RIG-I/Cardif ratio, and RIG-I/RNF125 ratio are shown. *Open columns* indicate SVR (n = 30), *shaded columns* indicate TR (n = 24), and *solid columns* indicate NVR (n = 20). *Error bars* indicate the standard error. The *P* values were analyzed by the Kruskal–Wallis test.

the first and the second phases of HCV dynamics (ISG15, first phase, $r = -0.5$, $P < .0001$; ISG15, second phase, $r = -0.3$, $P = .02$; USP18, first phase, $r = -0.5$, $P < .0001$; USP18, second phase, $r = -0.3$, $P = .01$).

Receiver Operator Characteristic Analysis

To determine the usefulness of these gene quantifications as predictors, receiver operator characteristic (ROC) analysis was conducted (Figure 3). The area under the ROC curve for the RIG-I/Cardif ratio, ISG15, and USP18 was 0.91, 0.90, and 0.91, respectively, suggesting that quantification of these gene transcripts is of use for the prediction of NVR (Table 2). In addition, this analysis also suggested that RIG-I/Cardif ratio would be more specific for prediction of NVR, whereas ISG15 and USP18 would be more sensitive (Table 2).

Multivariate Analysis

Multivariate analysis for factors that were available before initiating therapy indicated that a higher ratio of RIG-I/Cardif and higher expression of ISG15 were independent factors that were associated with NVR (Table 3). In this analysis, USP18 was excluded because of its strong correlation with ISG15.

Protein Levels of Cardif in the Liver

Because hepatic expression of Cardif mRNA was significantly lower in NVR patients than in SVR patients,

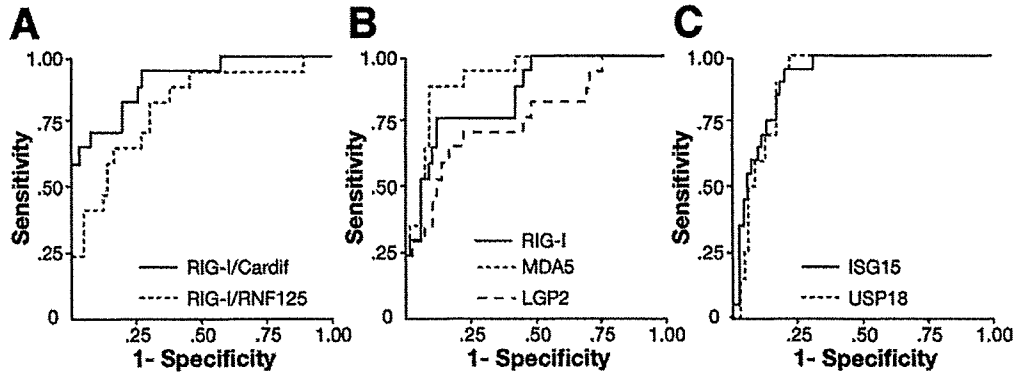

Figure 3. Receiver operator characteristic (ROC) curve for prediction of nonvirologic response. ROC curves were generated to compare (*A*) RIG-I/Cardif ratio (*solid line*) and RIG-I/RNF125 ratio (*shaded line*); (*B*) RIG-I (*solid line*), MDA5 (*shaded line*), and LGP2 (*dotted line*); and (*C*) ISG15 (*solid line*) and USP18 (*shaded line*).

Table 2. Area Under the ROC Curves, Sensitivity, Specificity, and Negative and Positive Predictive Values of Non-Virologic Responses

Variables	Az	95% CI	Cut-off	Sensitivity	Specificity	NPV[a]	PPV[b]
RIG-I	0.89	0.78–0.95	0.68	0.80	0.87	0.92	0.70
MDA5	0.92	0.86–0.98	0.84	0.82	0.89	0.93	0.74
LGP2	0.76	0.63–0.90	1.03	0.65	0.72	0.85	0.46
RIG-I/Cardif	0.91	0.84–0.99	0.88	0.75	0.91	0.91	0.75
RIG-I/RNF125	0.81	0.69–0.93	1.05	0.82	0.62	0.91	0.43
ISG15	0.91	0.85–0.97	0.36	0.90	0.81	0.96	0.64
USP18	0.90	0.84–0.96	0.67	0.90	0.83	0.96	0.67

[a]NPV, negative predictive value.
[b]PPV, positive predictive value.

we determined the basal protein expression levels of Cardif in the liver in NVR and SVR patients. Western blot analysis demonstrated a single Cardif product in all samples (Figure 4*A*). Similar to Cardif mRNA expression, mean Cardif expression in NVR patients was significantly lower than that in SVR (Figure 4*B*, $P = .01$). The cleavage product of Cardif, which has been reported by Loo et al,[23] was not detected in our analyses.

Transcriptional Responses to PEG-IFN-α-2b and Ribavirin Therapy in PBMC

Sequential analysis in response to PEG-IFN-α-2b and ribavirin demonstrated a rapid and strong induction of RIG-I, ISG15, and USP18 mRNA expression, which peaked 8 hours after PEG-IFN-α-2b administration (Figure 5). A greater fold change of these peak inductions was observed in SVR patients compared with NVR patients, although statistical significance was not achieved. In marked contrast, RNF125 expression profile in response to PEG-IFN-α-2b was triphasic, and consisted of (1) rapid and strong suppression peaked at 8 hours after administration, (2) increased 1.5- to 2-fold above baseline level during 24–48 hours after the administration, and (3) gradually decreased to baseline level (Figure 5). The rapid suppression and subsequent increase following PEG-IFN-α-2b administration tended to have a greater fold change in NVR patients compared with those in SVR patients. In contrast from RIG-I, ISG15, USP18, and RNF125, Cardif expression profile was relatively constitutive, and transcriptional response to PEG-IFN was weak (Figure 5).

Discussion

In the present study, we found that baseline expression levels of intrahepatic viral sensors and related regulatory molecules were significantly associated with the final virologic outcome in patients with chronic hepatitis C who were treated with PEG-IFN-α-2b and ribavirin combination therapy: up-regulation of RIG-I, MDA5, LGP2, ISG15, and USP18 and lower expression of Cardif and RNF125 could predict nonresponse to subsequent treatment with PEG-IFN-α-2b and ribavirin. The positive predictive value of a high ratio of expression of RIG-I to Cardif (>0.88) for NVR was the highest at a value of 0.75, and the negative predictive values of high expression of ISG15 (>0.36/internal control) and USP18 (>0.67/internal control) were the highest at values of both 0.96. These data may be of use in predicting clinical responses to the PEG-IFN-α and ribavirin combination before initiating therapy.

Table 3. Multivariate Analysis for the Factors Associated With Non-Virologic Response

Variable	Odds ratio	95% CI	*P* value
RIG-I/Cardif Ratio (by 0.1)	1.5	1.1–2.1	.008
RIG-I/RNF125 Ratio (by 0.1)	1.2	1.0–2.5	.1
ISG15 (by 0.1/internal control)	1.5	1.1–2.0	.01
Age (by 1 y)	1.0	0.9–1.1	.6
Platelet count (by $1 \times 10^4/\mu L$)	1.2	0.9–1.5	.07

Previously, large randomized controlled trials identified several pretreatment factors associated with the final virologic outcome, such as genotype, HCV RNA level, degree of fibrosis, age, body weight, ethnicity, and steatosis.[24] However, these findings lead us to believe that predicting the final virologic response before initiating PEG-IFN-α and ribavirin is difficult. Indeed, only age and platelet count were associated with the outcome in our patients with genotype 1b and a high viral load. Currently, the final response can be gauged only after treatment has been initiated. Although an early viral response at 12 weeks suggests the eventual outcome with 60%–90% accuracy,[25] a 12-week regimen is associated with adverse effects and is expensive. Therefore, this study investigated the baseline expression of genes involving innate immunity that may have significant effects on clinical outcomes.

In the present study, we demonstrated that RIG-I and MDA5 were inducible upon HCV infection and that expression of these intrahepatic positive viral sensors was up-regulated in NVR. In vitro studies have suggested that RIG-I and MDA5 play a pivotal role in the regulation of IFN production and augment the production of IFN via an amplification circuit. These results suggest that expression of RIG-I and MDA5 and related amplification system may be up-regulated by endogenous IFN at a higher baseline level in NVR patients. However, HCV elimination by subsequent exogenous IFN is insufficient

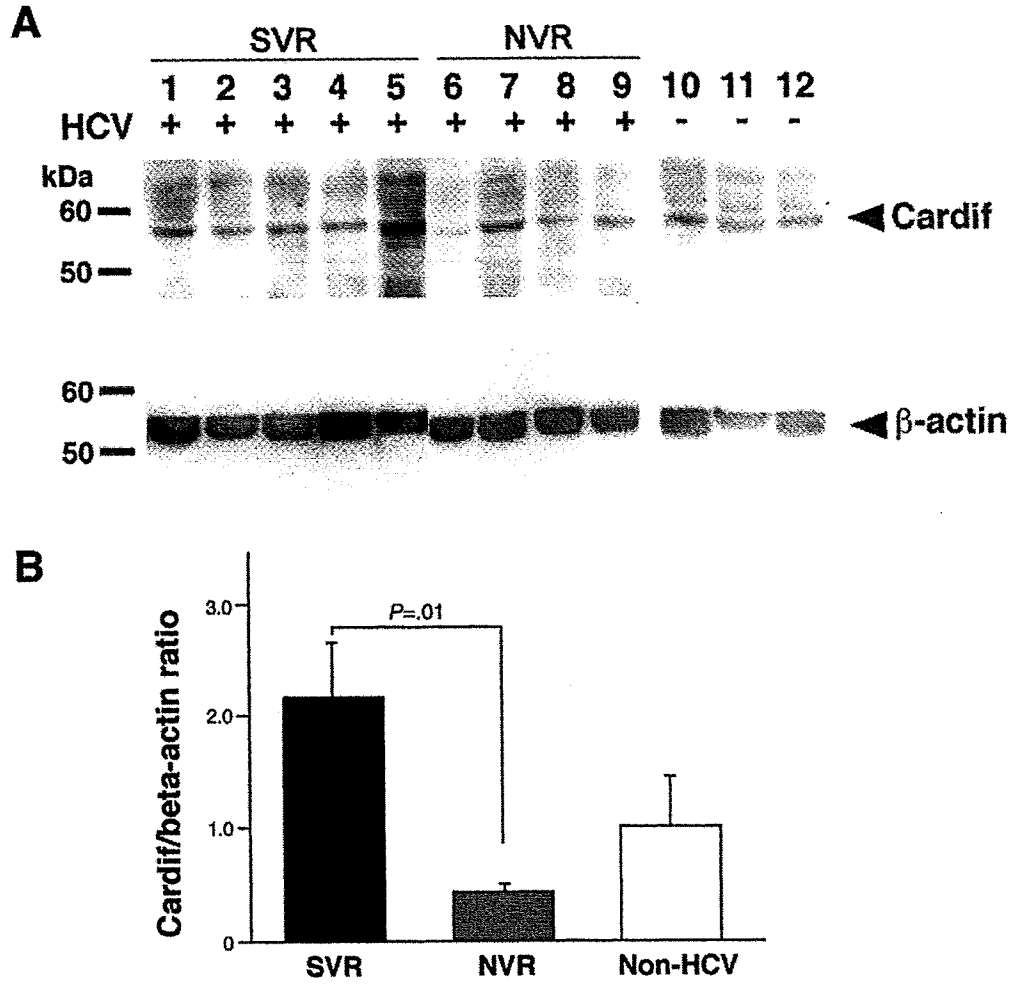

Figure 4. (*A*) Western blot analysis. Five lanes were SVR (*lanes 1–5*), 4 lanes were NVR (*lanes 6–9*), and 3 lanes were non-HCV control (*lanes 10–12*). Specific bands for Cardif and β-actin are indicated by *arrows*. (*B*) Expression level of Cardif protein normalized to β-actin in the liver biopsy specimens according to ultimate treatment response. *Error bars* indicate the standard error.

in these patients, suggesting that NVR patients may have adopted a different equilibrium in their immune response to the virus. In contrast to the expression of RIG-I and MDA5, Cardif mRNA, which was expressed in a relatively constitutive fashion, was significantly lower in NVR. Our ROC analysis highlights that lower expression of Cardif relative to that of RIG-I was one of the strongest predictors for NVR. Moreover, Western blot analysis further confirmed the down-regulation of Cardif in NVR patients, as demonstrated by its protein level. Because Cardif is one of the substantial target molecules of HCV evasion,[11,20] it is likely that Cardif expression is suppressed by HCV with resistant phenotype or is inadequate in NVR patients. Loo et al have demonstrated a Cardif cleavage product in 2 of 4 liver tissue samples of chronic HCV infection.[23] In our study, however, the Cardif cleavage product was not detected, presumably because the product could be unstable in vivo, resulting in rapid degradation. Although further studies are necessary to elucidate mechanisms of Cardif down-regulation, our findings of lower expression of Cardif in NVR suggested that the status of Cardif expression in the liver might have a significant effect on the ultimate outcome of antiviral treatment.

The antiviral effect brought by RIG-I/Cardif signaling is regulated by the coordination of negative and positive regulators. It has been shown that RNF125 functions as a negative regulator of RIG-I/Cardif signaling. RNF125 is an ubiquitin E3-ligase with activity against protein containing CARD domains, such as RIG-I, MDA5, and Cardif, and these ubiquitinated molecules undergo proteasomal degradation. In contrast, RNF125 do not have negative function against LGP2, a negative regulator of RIG-I signaling, because LGP2 lacks CARD domain. In contrast to RIG-I, RNF125 expression was rapidly suppressed by exogenous IFN; therefore, observed lower basal hepatic level of RNF125 in NVR could be explained by the suppressive effect of endogenous IFN, which may be up-regulated in NVR patients. Hence, RNF125 may constitute a negative regulatory circuit for IFN production and is responsible for responsiveness to PEG-IFN and ribavirin therapy.

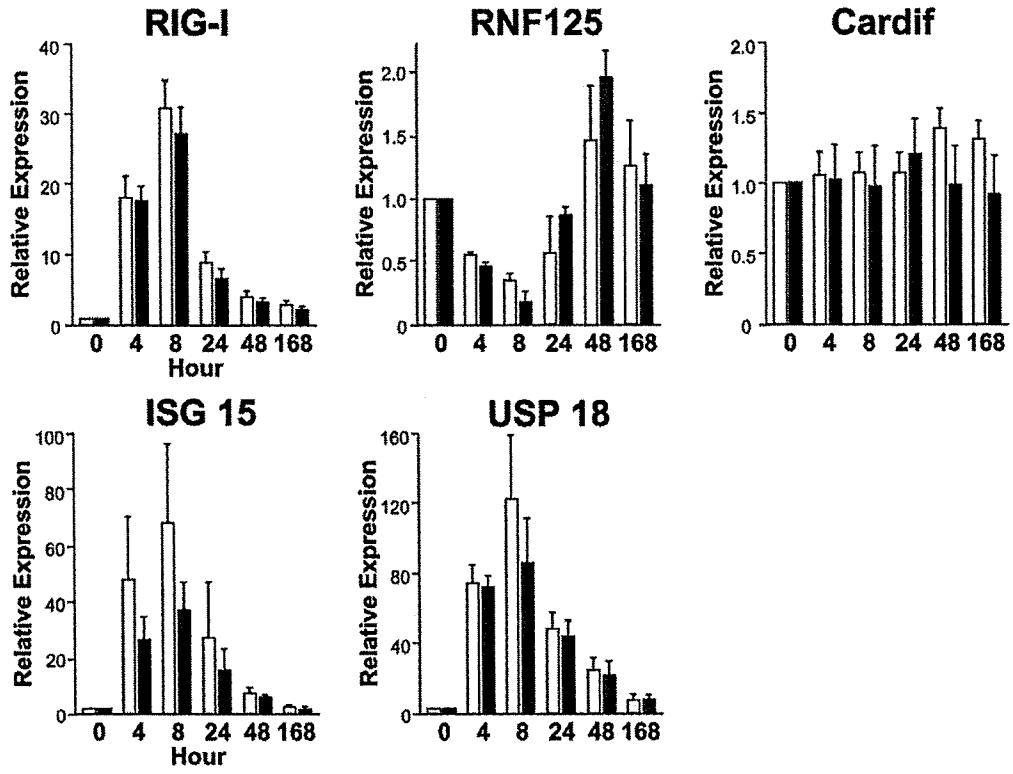

Figure 5. Transcriptional responses during PEG-IFN-α-2b and ribavirin therapy in PBMC (n = 14). *Open columns* indicate SVR (n = 7), and *solid columns* indicate NVR (n = 7). *Error bars* indicate the standard error. The *P* values determined by Mann–Whitney *U* test between 2 groups at 8 hours were as follows: RIG-I, *P* .3; RNF125, *P* .3; Cardif, *P* .7; ISG15, *P* .3; USP18, *P* .2.

It has been shown that RIG-I function is modified by ISG15 via ISGylation.[17] Consistent with our data, Chen et al identified 18 genes, including ISG15 and USP18, whose expression differed between responders and non-responders.[26] Interestingly, a recent study has shown that USP18 negatively regulates IFN signaling independently of its isopeptidase activity toward ISG15 by binding to the IFNAR2 receptor subunit and blocking the interaction between Janus kinase and the IFN receptor.[27] Moreover, the siRNA knockdown of USP18 in human cells has consistently been shown to potentiate the ability of IFN to inhibit HCV RNA replication.[28] Therefore, USP18 is suggested as a novel in vivo inhibitor of signal transduction pathways that are specifically triggered by type I IFN. Consistent with a role for USP18 in down-regulating the antiviral IFN response, we confirmed that up-regulation of USP18 was one of the factors predicting a lack of response to treatment with IFN.

The mechanism underlying the association of gene expression involving innate immunity with resistance to therapy is not well understood. Our human study with HCV patients treated by PEG-IFN and ribavirin highlights RIG-I/Cardif, RIG-I/RNF125, and ISG15/USP18, which is partly responsible for the clinical responsiveness to antiviral therapy. RIG-I signaling by viral pathogens may affect a wide variety of responses in not only innate but also acquired immunity. Our study is the first to demonstrate the potential relevance between molecules involving innate immunity and the clinical response to antiviral therapy.

In addition, sequential analysis of expression profile during PEG-IFN-α-2b and ribavirin treatment was also performed in this study. Lanford et al demonstrated transcriptional response to IFN-α in chimpanzee by genome microarray analysis, which included RIG-I, ISG15, and USP18.[29] An association of transcriptional response with early phase of virologic response has been also reported in PBMC or liver biopsy specimen.[30-32] We recently reported that the transcriptional double-stranded RNA-activated protein kinase response during treatment with PEG-IFN-α-2b and ribavirin was associated with the ultimate clinical response.[30] Similarly, the present study demonstrated a strong and rapid increase of RIG-I, ISG15, and USP18 mRNA in response to clinical PEG-IFN treatment especially in SVR patients, although few patients were available to achieve statistical significance between SVR and NVR. In marked contrast, transcriptional response of RNF125 exhibited a triphasic pattern. Rapid suppression seen in the first phase was presumably because of a negative regulatory effect of IFN. However, increase of RNF125 mRNA in the second phase, which tended to be grater in NVR, may be responsible for inhibiting RIG-I expression seen 8–48 hours after PEG-IFN-α-2b administration. Although limitations includ-

ing the use of PBMC and small sample size still deserve mention, the sequential expression profile during treatment may provide further valuable information regarding the prediction of the clinical response to the therapy and the mechanism of action of antiviral treatment.

In the present study, we have included patients with genotype 1b because it is imperative to designate a virologically homogeneous patient group to associate individual treatment responses with different gene expression profiles that direct innate immune responses. We have preliminarily studied genotype 2 patients and found that Cardif and RNF125 gene expression levels in NVR patients were significantly lower than those with SVR patients ($P = .03$ and $P = .04$, respectively) and that RIG-I/Cardif and RIG-I/RNF125 ratios were significantly higher in NVR patients ($P = .02$ and $P = .009$, respectively, see Supplementary Figure 2 online at www.gastrojournal.org). These findings suggest that the differences in gene expression profiles between SVR and NVR were almost identical to those demonstrated in patients with genotype 1b. However, the correlation between treatment responses in all the genotypes and the different status of innate immune responses needs to be explored. Further studies may be necessary to clarify this issue.

In conclusion, the results of the present study offer potentially important clinical implications for patients with chronic hepatitis C who are treated with PEG-IFN-α and ribavirin. Quantifying hepatic gene expression of the RIG-I/Cardif system, including its regulators before treatment, is useful in identifying patients who are at a higher risk for NVR. The data from these assays can provide valuable information that may influence the decision about the treatment strategy in each individual patient. Finally, this clinical human study demonstrates the potential relevance of the molecules involving innate immunity to the clinical response to therapy. Our data will help understand the pathogenesis of HCV resistance and development of new antiviral therapy targeted toward the innate immune system.

Supplementary Data

Note: To access the supplementary material accompanying this article, visit the online version of *Gastroenterology* at www.gastrojournal.org, and at doi: 10.1053/j.gastro.2008.02.019.

References

1. Kiyosawa K, Sodeyama T, Tanaka E, et al. Interrelationship of blood transfusion, non-A, non-B hepatitis and hepatocellular carcinoma: analysis by detection of antibody to hepatitis C virus. Hepatology 1990;12:671–675.
2. Manns MP, McHutchison JG, Gordon SC, et al. Peginterferon alfa-2b plus ribavirin compared with interferon alfa-2b plus ribavirin for initial treatment of chronic hepatitis C: a randomised trial. Lancet 2001;358:958–965.
3. Fried MW, Shiffman ML, Reddy KR, et al. Peginterferon alfa-2a plus ribavirin for chronic hepatitis C virus infection. N Engl J Med 2002;347:975–982.
4. Hadziyannis SJ, Sette HJ, Morgan TR, et al. PEGASYS International January 2006 American Gastroenterological Association 253 Study Group. Peginterferon-α-2a and ribavirin combination therapy in chronic hepatitis C: a randomized study of treatment duration and ribavirin dose. Ann Intern Med 2004;140:346–355.
5. Zeuzem S, Pawlotsky JM, Lukasiewicz E, et al. DITTO-HCV Study Group. International, multicenter, randomized, controlled study comparing dynamically individualized versus standard treatment in patients with chronic hepatitis C. J Hepatol 2005;43:250–257.
6. Berg T, von Wagner M, Nasser S, et al. Extended treatment duration for hepatitis C virus type 1: comparing 48 versus 72 weeks of peginterferon-alfa-2a plus ribavirin. Gastroenterology 2006;130:1086–1097.
7. Biron CA. Initial and innate responses to viral infections—pattern setting in immunity or disease. Curr Opin Microbiol 1999;2:374–381.
8. Gale M Jr, Foy EM. Evasion of intracellular host defence by hepatitis C virus. Nature 2005;436:939–945.
9. Yoneyama M, Kikuchi M, Natsukawa T, et al. The RNA helicase RIG-I has an essential function in double-stranded RNA-induced innate antiviral responses. Nat Immunol 2004;5:730–737.
10. Yoneyama M, Kikuchi M, Matsumoto K, et al. Shared and unique functions of the DExD/H-box helicases RIG-I, MDA5, and LGP2 in antiviral innate immunity. J Immunol 2005;175:2851–2858.
11. Meylan E, Curran J, Hofmann K, et al. Cardif is an adaptor protein in the RIG-I antiviral pathway and is targeted by hepatitis C virus. Nature 2005;437:1167–1172.
12. Kawai T, Takahashi K, Sato S, et al. IPS-1, an adaptor triggering RIG-I- and Mda5-mediated type I interferon induction. Nat Immunol 2005;6:981–988.
13. Seth RB, Sun L, Ea CK, et al. Identification and characterization of MAVS, a mitochondrial antiviral signaling protein that activates NF-κB and IRF 3. Cell 2005;122:669–682.
14. Xu LG, Wang YY, Han KJ, et al. VISA is an adapter protein required for virus-triggered IFN-β signaling. Mol Cell 2005;19:727–740.
15. Rothenfusser S, Goutagny N, DiPerna G, et al. The RNA helicase Lgp2 inhibits TLR-independent sensing of viral replication by retinoic acid-inducible gene-I. J Immunol 2005;175:5260–5268.
16. Arimoto K, Takahashi H, Hishiki T, et al. Negative regulation of the RIG-I signaling by the ubiquitin ligase RNF125. Proc Natl Acad Sci U S A 2007;104:7500–7505.
17. Zhao C, Denison C, Huibregtse JM, et al. Human ISG15 conjugation targets both IFN-induced and constitutively expressed proteins functioning in diverse cellular pathways. Proc Natl Acad Sci U S A 2005;102:10200–10205.
18. Schwer H, Liu LQ, Zhou L, et al. Cloning and characterization of a novel human ubiquitin-specific protease, a homologue of murine UBP43 (Usp18). Genomics 2000;65:44–52.
19. Malakhov MP, Malakhova OA, Kim KI, et al. UBP43 (USP18) specifically removes ISG15 from conjugated proteins. J Biol Chem 2002;277:9976–9981.
20. Li XD, Sun L, Seth RB, et al. Hepatitis C virus protease NS3/4A cleaves mitochondrial antiviral signaling protein off the mitochondria to evade innate immunity. Proc Natl Acad Sci U S A 2005;102:17717–17722.
21. Nakagawa M, Sakamoto N, Tanabe Y, et al. Suppression of hepatitis C virus replication by cyclosporin A is mediated by blockade of cyclophilins. Gastroenterology 2005;129:1031–1041.
22. Asahina Y, Izumi N, Uchihara M, et al. A potent antiviral effect on hepatitis C viral dynamics in serum and peripheral blood mononuclear cells during combination therapy with high-dose daily

interferon α plus ribavirin and intravenous twice-daily treatment with interferon β. Hepatology 2001;34:377–384.
23. Loo YM, Owen DM, Li K, et al. Viral and therapeutic control of IFN-β promoter stimulator 1 during hepatitis C virus infection. Proc Natl Acad Sci U S A 2006;103:6001–6006.
24. Dienstag JL, McHutchison JG. American Gastroenterological Association technical review on the management of hepatitis C. Gastroenterology 2006;130:231–264.
25. National Institutes of Health. National Institutes of Health Consensus Development Statement: management of hepatitis. Hepatology 2002;36(Suppl 1):S3–S20.
26. Chen L, Borozan I, Feld J, et al. Hepatic gene expression discriminates responders and nonresponders in treatment of chronic hepatitis C viral infection. Gastroenterology 2005;128:1437–1444.
27. Malakhova OA, Kim KI, Luo JK, et al. UBP43 is a novel regulator of interferon signaling independent of its ISG15 isopeptidase activity. EMBO J 2006;25:2358–2367.
28. Randall G, Chen L, Panis M, et al. Silencing of USP18 potentiates the antiviral activity of interferon against hepatitis C virus infection. Gastroenterology 2006;131:1584–1591.
29. Lanford RE, Guerra B, Lee H, et al. Genomic response to interferon-α in chimpanzees: implications of rapid down-regulation for hepatitis C kinetics. Hepatology 2006;43:961–972.
30. Asahina Y, Izumi N, Umeda N, et al. Pharmacokinetics and enhanced PKR response in patients with chronic hepatitis C treated with pegylated interferon α-2b and ribavirin. J Viral Hepat 2007;14:396–403.
31. Taylor MW, Tsukahara T, Brodsky L, et al. Changes in gene expression during pegylated interferon and ribavirin therapy of chronic hepatitis C virus distinguish responders from nonresponders to antiviral therapy. J Virol 2007;81:3391–3401.
32. Feld JJ, Nanda S, Huang Y, et al. Hepatic gene expression during treatment with peginterferon and ribavirin: identifying molecular pathways for treatment response. Hepatology 2007;46:1548–1563.

Received August 30, 2007. Accepted January 31, 2008.

Address requests for reprints to: Namiki Izumi, MD, PhD, Chief, Department of Gastroenterology and Hepatology, Musashino Red Cross Hospital, 1-26-1 Kyonan-cho, Musashino-shi, Tokyo 180-8610, Japan. e-mail: nizumi@musashino.jrc.or.jp; fax: (81) 422-32-9551.

Supported by grants from the Miyakawa Memorial Research Foundation; the Japanese Ministry of Education, Culture, Sports, Science and Technology; and the Japanese Ministry of Welfare, Health and Labor.

Financial disclosures: The authors who participated in this study have had no affiliation with the manufacturers of the drugs involved either in the past or in present and have not received funding from the manufacturers to conduct this research.